

# ALS (AIRBORNE LIDAR) ACCURACY: CAN POTENTIAL LOW DATA QUALITY OF GROUND POINTS BE MODELLED/DETECTED? CASE STUDY OF 2016 LIDAR CAPTURE OVER AUCKLAND, NEW ZEALAND

**Gabriela Olekszyk**

---

2022  
Department of  
Physical Geography and Ecosystem Science  
Centre for Geographical Information Systems  
Lund University  
Sölvegatan 12  
S-223 62 Lund  
Sweden



# ALS (Airborne Lidar) accuracy: Can potential low data quality of Lidar ground points be modelled/detected based on recorded point cloud characteristics? Case study of 2016 Lidar capture over Auckland, New Zealand

---

Gabriela Olekszyk (2022).

Master's degree thesis, 30 credits in Master in Geographical Information Science  
Department of Physical Geography and Ecosystem Science, Lund University

Supervisors

Hongxiao Jin

Department of Physical Geography and Ecosystem Science  
Lund University

Ning Zhang

Department of Physical Geography and Ecosystem Science  
Lund University

## Acknowledgements

I want to thank my supervisors Hongxiao Jin and Ning Zhang for their support during my work on this thesis. Their help and suggestions have been trully valuable while completing this project. I have apprieciated both your patience and flexibility to guide me whilst living in dramatically different time zones.

I would also like to acknowledge Sam Hackett, who has given me insiparion for this thesis. His expertise has helped me both to achieve my academic goals and with my continued professional developemnt.

I want to also thank the examination commitee, who helped shape this final paper.

Finally, I'd like to thank my partner Will for motivating me, supporting me and being there for me in tough moments.

# Abstract

Lidar (Light Detection and Ranging) data is becoming more widely available and accessible. In many cases, it can be obtained free of charge from government agencies or local councils. In order to effectively use it in applications that require high precision, the data must be carefully studied, and sometimes verified with high precision terrestrial survey, to avoid issues introduced by potentially low point cloud accuracy.

Accuracy of Lidar data is influenced by multiple factors, such as instrument position and internal errors, distance to measured surface, errors in point detection, wrong classification or complex, sloping terrain.

This research focuses on analysing if recorded point characteristics, as well as some point cloud shape characteristics, show a relationship with poor data accuracy.

Data used in this study was obtained for and distributed by Auckland Council in New Zealand. The available point cloud covers a large portion of Auckland and its surroundings.

LAStools software has been used to manipulate the point cloud and extract various characteristics for 5m by 5m grid cells. Tested variables included: The number of present classes in a cell, the density of ground points (also after applying thinning algorithms), the height range and standard deviation of ground points, the intensity range, the average value and standard deviation, the average number of returns, the average scan angle, and the slope. Correlation analysis and multiple regression have been performed and no significant relationship was found between the tested variables and data accuracy using this research paper's methodology. When comparing ground and low vegetation classes, some point cloud characteristics trends have been found, however, these are not suitable to aid with misclassification detection.

Failure to detect meaningful relationships between recorded point cloud characteristics and accuracy or misclassification errors does not definitely mean that there are none. Different methods could lead to more promising outcomes.

# Contents

|   |     |
|---|-----|
| Acknowledgements .....  | iii |
| Abstract .....  | iv  |
| Contents .....  | v   |
| Figures .....   | vi  |
| Tables.....   | vii |
| 1. Introduction.....  | 1   |
| 2. Background.....  | 3   |
| 2.1 Lidar, ALS and basic properties .....   | 3   |
| 2.2 ALS Accuracy.....   | 6   |
| 3. Methodology .....  | 9   |
| 3.1 Study Area and Data.....  | 9   |
| Auckland, New Zealand .....   | 9   |
| 2016/2017 Lidar Data .....  | 9   |
| Point cloud data.....   | 10  |
| 3.2 Software .....  | 11  |
| 3.3 Data Investigation.....   | 11  |
| Tiles: point source IDs, intensity values and classification.....   | 11  |
| 3.4 Data selection.....   | 16  |
| 3.5 Data processing / manipulation .....  | 18  |
| Workflow overview .....   | 18  |
| 4. Data analysis.....   | 23  |
| 4.1 Analysis of relationship between various Lidar point characteristics and the measure<br>of accuracy: correlation and regression ..... | 23  |
| Correlation.....  | 23  |
| Multiple regression.....  | 24  |
| 4.2 Additional analysis.....  | 24  |
| 5. Results .....  | 25  |
| 5.1 Correlation.....  | 25  |
| 5.2 Multiple regression.....  | 28  |
| 5.3 Additional analysis.....  | 29  |
| 6. Discussion and conclusions .....   | 33  |
| 6.1 Research shortcomings .....   | 33  |
| 6.2 Further research .....  | 34  |
| 6.3 Final word .....  | 35  |

|   |    |
|---|----|
| 7. References.....                        | 37 |
| Appendix A .....                          | 39 |
| Appendix B.....                           | 41 |
| Appendix C.....                           | 42 |
| Displaz.....                              | 42 |
| FugroViewer .....                         | 42 |
| LAStools .....                            | 43 |
| Notepad ++ .....                          | 44 |
| Windows PowerShell.....                   | 44 |
| FME.....                                  | 44 |
| ArcGIS Pro.....                           | 45 |
| Microsoft Excel .....                     | 46 |
| Licensing .....                           | 46 |
| Other notes.....                          | 46 |
| Appendix D .....                          | 47 |
| Workflow – ArcGIS Pro .....               | 47 |
| Workflow – LAStools – Methodology 1 ..... | 47 |
| Workflow – LAStools – Methodology 2 ..... | 57 |
| Workflow – FME .....                      | 57 |
| Appendix E.....                           | 60 |

## Figures

|  |    |
|--|----|
| Figure 1: Full waveform return.....  | 4  |
| Figure 2: Point cloud symbolised based on recorded point properties. ....                    | 6  |
| Figure 3: Scanning geometry.....   | 7  |
| Figure 4: Auckland Lidar 2016 survey capture extent.....                                     | 9  |
| Figure 5: Sample LAZ file and corresponding tile information .....                           | 10 |
| Figure 6: BA31_0437_2016: LAS Classification. ....   | 12 |
| Figure 7: BA31_0437_2016: Intensity. ....  | 12 |
| Figure 8: BA31_0437_2016: Point source. ....   | 13 |
| Figure 9: BA31_0437_2016 slice – class.....  | 13 |
| Figure 10: BA31_0437_2016 slice – intensity.. ....   | 13 |
| Figure 11: AZ30_4745_2016.....   | 15 |
| Figure 12: Test areas locations .....  | 16 |
| Figure 13: Test areas examples .....   | 17 |
| Figure 14: Methodology 1 overview chart .....  | 18 |
| Figure 15: Methodology 2 overview chart .....  | 19 |
| Figure 16: LAStools workflow (Methodology1).....   | 20 |
| Figure 17: LAStools workflow (Methodology 2).....  | 20 |
| Figure 18: Scatter plot: Trends of thinned point counts. No clear relationship visible. .... | 26 |

|  |    |
|--|----|
| Figure 19: Scatter plot: Trends of class variety. No clear relationship visible..... | 27 |
| Figure 20: Scatter plot: Trend between class variety and thinned point count.....    | 27 |
| Figure 21: Additional analysis.....  | 29 |
| Figure 22: Additional analysis.....  | 29 |
| Figure 23: Additional analysis.....  | 30 |
| Figure 24: Class 2 (ground) and Class 3 (low vegetation) comparison.....             | 31 |
| Figure 25: Displaz .....   | 42 |
| Figure 26: FugroViewer .....   | 43 |
| Figure 27: example bat file executing LAStools - "lasoverlap" .....                  | 44 |
| Figure 28: FME.....  | 45 |
| Figure 29: ArcGIS Pro.....   | 45 |
| Figure 30: Tiles intersecting test areas - ArcGIS Pro table view .....               | 47 |
| Figure 31: 1_CopyLaz.bat .....   | 48 |
| Figure 32: 2_ClipLazByShp.bat .....  | 48 |
| Figure 33: 3_CreateDEMs_orig.bat .....   | 49 |
| Figure 34: 4_SplitFlightLines.bat .....  | 50 |
| Figure 35: 5_Reclassify.bat.....   | 50 |
| Figure 36: 6_CreateDEMs_FlightlinesReclass.bat .....                                 | 51 |
| Figure 37: Adaptive thinning supporting graphic.....                                 | 51 |
| Figure 38: 7_AdaptiveThin_01_05.bat .....  | 52 |
| Figure 39: 8_LasGrid_PCount_Orig_5.bat.....  | 52 |
| Figure 40: 8_LasGrid_PCount_Thin01_5.bat.....  | 53 |
| Figure 41: 8_Las2DEM_Slope.bat.....  | 53 |
| Figure 42: 8_LasGrid_ScanAngleAvg.bat.....   | 54 |
| Figure 43: 8_LasGrid_ClassVar.bat .....  | 54 |
| Figure 44: 8_LasGrid_RetNumAvg.bat .....   | 55 |
| Figure 45: 8_LasGrid_HRange.bat .....  | 55 |
| Figure 46: 8_LasGrid_HStdDev.bat.....  | 56 |
| Figure 47: 8_LasGrid_IntensityRange.bat .....  | 56 |
| Figure 48: 8_LasGrid_IntensityAvg.bat .....  | 57 |
| Figure 49: 8_LasGrid_IntensityStdDev.bat .....                                       | 57 |
| Figure 50: FME workflow Methodology 1 .....  | 58 |
| Figure 51: FME workbench (Methodology 1).....  | 58 |
| Figure 52: FME workflow Methodology 2 .....  | 59 |
| Figure 53: FME workbench (Methodology 2).....  | 59 |

## Tables

|                                       |    |
|---------------------------------------|----|
| Table 1: Point cloud classes.....     | 11 |
| Table 2: Correlation coefficient..... | 25 |
| Table 3: Multiple regression.....     | 28 |





# 1. Introduction

Using Lidar (Light Detection and Ranging) data can significantly increase the quality and decrease the cost of many projects with comparison to traditional survey methods that are labor intensive, expensive and time consuming. Larger scale survey campaigns can utilize remote sensing technologies, such as photogrammetry or Lidar, that allow faster data acquisition for big areas. The latter has an advantage over photogrammetric methods - it can penetrate through vegetation.

When using Lidar data, it is crucial to have a better understanding of what levels of accuracy can be expected. Although government agencies would provide expected accuracies, they are typically stated uniformly for the full dataset, and the user always must acknowledge that no warranty about the accuracy and completeness is given. It could be beneficial to develop methods for evaluating data accuracy so that necessary cautions can be taken in areas with lower accuracy.

In the case of the 2016 Auckland Lidar dataset, it has been noted that there is a significant offset in elevation between different Lidar data captures in some areas, while in others the points from different passes show consistent (matching) height (source: Sam Hackett, Associate Surveyor / Mobile Mapping Manager, Wood & Partners Consultants Ltd , during data QA process) . Lidar can penetrate through vegetation; but low and dense vegetation affects the accuracy of resulting point cloud. Another cause of discrepancy may be the angle at which data was captured (which is dependent on both: terrain characteristics and offset from flight paths' centres). There have been studies examining factors that influence survey accuracy – Iordan and Popescu (2015) investigated the influences of varying types of topography (such as mountainous, rolling, or flat terrain) on elevation surface accuracy and found that there is a relationship between the two. They also assessed the difference in accuracy of measurements across different land cover types.

In this research, an effort has been made to model accuracy of ground measurements (the last laser return) by investigating data and determining if accuracy can be predicted based on certain characteristics, such as recorded points intensity, or density and height variations between ground points.



## 2. Background

### 2.1 Lidar, ALS and basic properties

Lidar, which stands for Light Detection and Ranging, is a surveying method that uses laser pulses to determine the location of measured surfaces. Lidar is an active remote sensing technique and relies on an instrument emitting laser pulses and then recording them as they return after bouncing off the surface of objects that are being surveyed. For terrestrial laser scanning, when the instrument is stationary and its position and orientation is often known before the scan commences (but can also be determined during post processing), the method behind computing surveyed points locations is relatively straight forward. By measuring the time that it took for a laser beam to return and combining this information with the instrument's position and direction at which the laser has been emitted, the instrument is able to calculate three dimensional coordinates of a point on the surface. Computations are more complex for surveying techniques that take advantage of mobile platforms. These include terrestrial mobile laser scanning (when a scanner is mounted on a moving vehicle on a ground, for example on a car) and ALS – Airborne Laser Scanning (when scanning is done from a plane or UAV – unmanned aerial vehicle). Although the measurement principle is the same, it is harder to determine the location of instrument to a required accuracy – because of this, GPS and IMU units must be part of the system. An on-board processing unit derives and records the georeferenced points in real time by combining all before mentioned information. This form of data collection is very fast and enables a system to record large quantities of data in a very short time. The output of Lidar survey is a point cloud (a dataset that consists of a large amount of recorded x, y, z coordinates, together with metadata).

While many laser-scanning instruments record one point per emitted pulse, modern ALS uses full-waveform information to record multiple points, as portions of signal are returned at different times. When a laser pulse is released, it does not stay the same width while it travels towards the surveyed topography, but rather forms a diffraction cone. Because of a significant distance between the laser scanning apparatus and the surveyed objects, the footprint of a laser beam is large by the time it hits the surface -around 200-300mm depending on the height above the ground and an incident angle. At this size, it is likely that portions of the beam will intersect with multiple objects at potentially different heights (for example, leaves and branches of a tree and the ground below). Portions of the beam hitting higher objects will return earlier to the scanning unit than portions bouncing off lower objects, while if the beam penetrates to the ground (and then finds its way back to the measuring instrument), it becomes the last return of a laser pulse. Therefore, the return signal received at the ALS processing unit, is not a single pulse per emitted pulse, but rather a waveform of different signal intensity distributed across the time. Algorithms are used to classify the waveform in a way to derive time at waves peaks and compute distinct points using this information. Because of this property, airborne laser scanning allows to penetrate through vegetation and acquire points both on the tree canopy as well as on the objects below (this, naturally, depends on the vegetation characteristics, such as the density of the foliage).

This penetrability is a major advantage of ALS over photogrammetric methods, which do not have this potential. Figure 1 (below) shows the representation of a full-waveform return, (figure is based on Fig.3 in “Full-waveform topographic lidar: State-of-the-art” by Mallet C., Bretar F.). The authors explain the methodology of determining 3D points based on received waveform peaks, and they also point out the relationship between the size of a laser beam and penetrability. A larger laser footprint (B on the figure below) is more likely to penetrate to the ground, however, horizontal precision is lower compared to a narrow footprint (A on the figure below).



Figure 1: Full waveform return. On the left, narrow laser beam (A) records two apple tree branches and a lavender bush. It does not penetrate to the ground. On the right, wide laser beam (B) records multiple tree brunches, 2 types of lavender bushes, and the ground.

Intensity of the laser return signal used to derive points at peaks, is typically recorded against each point and may be further used to aid with classification of the data as well as with point cloud quality assessment: “(...) the exploitation of the geometric information has been coupled by the use of laser intensity, which may provide additional data for multiple purposes. This option has been emphasized by the availability of sensors working on different wavelength, thus able to provide additional information for classification of surfaces and objects. Several applications of monochromatic and multi-spectral LiDAR data have been already developed in different fields: geosciences, agriculture, forestry, building and cultural heritage. The use of intensity data to extract measures of point cloud quality has been also developed.” (Scaioni et al., 2018).

Research into using intensity information for quality assessment is very complex, and includes studies of laser scanners stochastic characteristics, studies of distance influence, studies of nighttime versus daytime survey and more. Generally, intensity depends on the survey configuration, objects’ radiometric characteristics, and return number. This means that the same object can be recorded with different intensity under different conditions. For example, two different instruments used for the survey, can

capture that same object showing different intensity. The same surface with different moisture content (in dry condition versus after rain) can be recorded with different intensity. However, within one point cloud, recorded at one time, with one instrument, intensity within object is more homogenous. Because of it, when examining point clouds colorized by intensity it is easy to distinguish different features.

Based on the knowledge that different objects can be recorded with different intensity, and thus larger intensity variations within one class and one area can point to wrong classification, has been explored in this research. When examining intensity characteristics in this project, it is done so on a single flight basis and not on a point cloud combined from multiple flight passes, to avoid the effects of variation in moisture content, possibly different instrument and/or settings used etc. Moreover, only points recorded by first laser beam return are used since return number has large effect on recorded intensity.

Displaz software (<http://c42f.github.io/displaz/>, developed by Christopher J. Foster and others) was used to demonstrate how a sample point cloud looks like, together with some recorded point characteristics. Figures below show point cloud (RPC\_AZ31\_4803\_2016.laz sourced from Auckland Council), symbolised by:

- a) Return number: peaks of trees and ground on open spaces is a first return – fresh green, lower vegetation below tree canopy and ground below vegetation are later returns
- b) Reversed return number (starting with last return): ground – last return is displayed in fresh green, regardless if vegetation above is present or not (unless the laser did not penetrate to the ground)
- c) Number of returns for the laser pulse that was used to derive any point: open spaces where only one return has been recorded are shown in fresh green, while areas where laser pulse has been separated into many peaks are shown in different colours (orange and less visible military green).
- d) Intensity: amongst other factors, intensity is related to the number of returns and how much energy bounced back and was detected in form of a peak of the full waveform and thus prompted the creation of point at specific location – it can be seen that under vegetated areas, ground points are shown in dark colour, which means that a small amount of laser pulse penetrated to the last recorded surface. Typically, 90% of total reflected signal power is consumed within the first two returns (2009, Mallet C., Bretar F.).

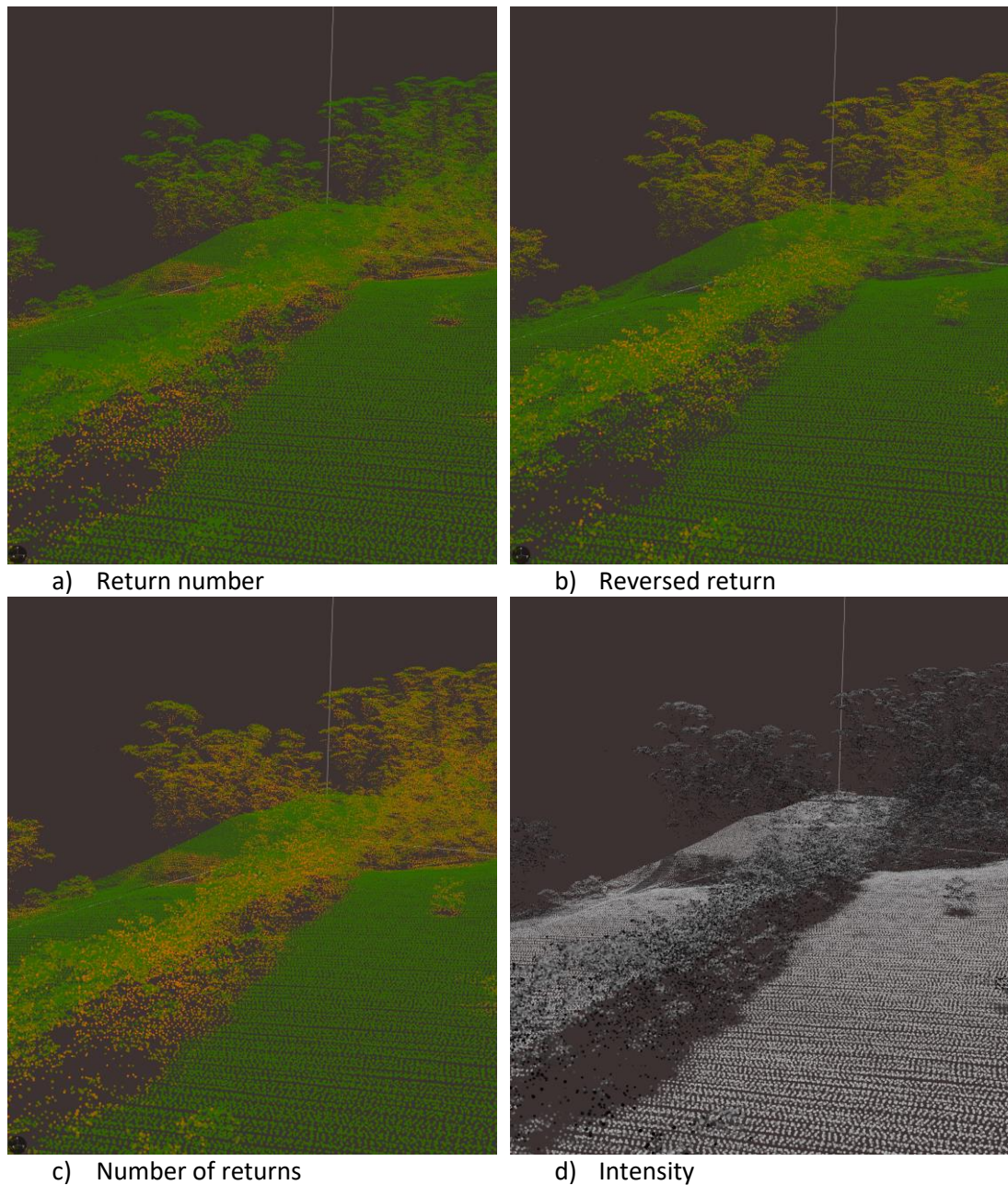


Figure 2: Point cloud symbolised based on recorded point properties. A – colour based on a return number (first return – green, second return – orange, third return – military green). B – colour based on a reversed return (last return – green, second last return – orange, third last return – military green). C – colour based on a number of returns (one return – green, all points collected by a laser beam that had two returns – orange, all points collected by a laser beam that had three returns – military green). D – colour based on intensity (points of higher intensity – lighter shades of grey, points of lower intensity – darker shades of grey).

## 2.2 ALS Accuracy

ALS has lower accuracy than terrestrial laser scanning, due to several factors that influence the errors magnitude. Firstly, there may be some discrepancy between computed and true position and bearing of instrument as well as internal instrument error. Secondly, significantly larger distance between the instrument and measured surface causes the accuracy deterioration. A slight error in a measurement angle is

amplified over a longer distance. Due to a distance and the size of the laser beam footprint (as explained in previous section), horizontal accuracy cannot be better than the size of this footprint (since it is not known which portion of echo came from what direction within the narrow laser beam cone). Both horizontal and vertical accuracies are affected, as explained in “Accuracy estimation for laser point cloud including scanning geometry” (Schaer et al., 2007), because the incidence angle between laser beam and the terrain reflects in footprint size and power distribution. This is especially a critical problem with incidence angles far from the surface normal, that result in significantly larger laser beam footprints, as shown in Figure 3. Finally, there are errors in point detection (analysis of echo peaks, disregarding noise) and classification that are related to the full-waveform approach, which is not commonly used in terrestrial laser scanning. Although not entirely based on point accuracy itself, there is a problem of ground points accuracy. The ground data – last returns, may be subject to error in terms of wrong classification (when point representing object above the ground, such as vegetation, is classified as ground) as well as wrong echo peak detection (when vegetation just above the ground is very dense). Ground points vertical accuracy is the most important, as these points are used to generate Digital Elevation Models (DEMs), used in variety of applications.



Figure 3: Scanning geometry. Figure demonstrates how incidence angle is a product of scanning angle and terrain slope. Surveyed point (yellow star) is positioned between the flight path centres of A and B. Because of the terrain slope, incidence angle for B is close to  $90^\circ$ , while the incidence angle for A is obtuse, far from normal.

As outlined in the ASPRS (American Society for Photogrammetry and Remote Sensing) guidelines, the high accuracy products are required for 5 primary fields: marine navigation and safety, stormwater and floodplain management, wetlands and ecologically sensitive areas management, infrastructure management in urban areas, and, lastly, special engineering applications. In other applications, users may be able to successfully utilize data of lower vertical accuracy. For this reason, guidelines propose several accuracy classes, that datasets can fall into. The classes help the end user to determine usability of data quoting different types of accuracies (horizontal, vertical, RMSE etc.) for a specific purpose. Although the idea is simple, in reality one ALS dataset can consist of points with significantly varying vertical accuracies – this is especially true for large datasets covering a variety of surface types. In these circumstances, guidelines suggest reporting separate accuracies. Three cases have been distinguished, that can be the basis of splitting data into different quality portions: the continuity of data collection and processing (dependent on equipment and collection/computing methods), topographic variation (terrain slope), and ground cover variation (bare ground, tall or short vegetation etc.). ASPRS guidelines suggest that unless there is a specific reason, the accuracy can be based on data collected over open terrain. This is referred to as fundamental vertical accuracy. While testing data accuracy over other ground covers is not required, points collected over non-bare ground are then just known to be of lower (but not well specified) quality. If accuracy is required to be specifically quoted for different land cover categories (which should be determined by the customer), then accuracy testing needs to be designed with this in mind (by ensuring adequate check points have been included). Accuracy specific to different land cover categories (or their combinations) is referred to as supplemental or consolidated accuracy, and should be determined using the 95<sup>th</sup> percentile method rather than the RMSE (as is the case for fundamental accuracy), due to the error not following the normal distribution (ASPRS Guidelines Vertical Accuracy Reporting for Lidar Data V1.0). Even with splitting accuracy testing this way, data collectors and users may find that there may be further variation in point cloud quality. The recommendation in “ASPRS Accuracy Standards for Digital Geospatial Data” (March, 2015) is to develop polygons indicating low confidence areas. These should be created based on nominal ground point density, raster cell size, search radius and minimum mapping unit (as explained in appendix C.8 of the guidelines).

ASPRS recommendation focuses mainly on ground point density to determine data of lower accuracy within non-bare ground land cover areas. As outlined previously, this is not the only indication of possible deterioration of data quality. Schaer et al. (2007) propose a q-value – a quality indicator for individual points within the point cloud, based on accumulation of random errors and scanning geometry analysis. Perhaps there are other indicators of lower data quality that can be further explored. In this thesis, reflectance and roughness of ground point data will be examined amongst others.



## 3. Methodology

### 3.1 Study Area and Data

#### Auckland, New Zealand

The study area covers a wide region including Auckland and surrounding rural areas, on New Zealand's North Island. During the Lidar aerial survey that took place in 2016 and 2017, point cloud data has been recorded, covering extents of land under the governance of Auckland Council (see appendix E). This land consists of the urban area of New Zealand's largest city, as well as areas to the east and west (limited by water boundary), to the north (up to and including Wellsford), the south (including Hunua Ranges and Pukekohe), and few offshore islands, including Rangitoto, Waiheke, Chamberlins, Kawau, Little, and Great Barrier Islands.

#### 2016/2017 Lidar Data

The digital mapping dataset used for this project has been collected for, and distributed by, Auckland Council in New Zealand. It consists of a few products: raw point clouds, ground point clouds, above ground point clouds, DEM, Digital Surface Model (DSM), contours, and imagery. Supporting materials including a license, information about data (see appendix A) and a tile layout shapefile that references point cloud data are also supplied. Data carries the creative commons international license (attached in appendix B). In this project, raw point clouds will be used as a primary object of study, however, other products provided with the same dataset (imagery and DEM) will also be used for reference and analysis.

Data has been collected between November 2016 and June 2017.

Raw point cloud data, distributed by Auckland Council, comes in LAS v1.2 format and covers a large area of Auckland city and its surroundings (Figure 4 – red area). Because of the size of area – over 670 000 ha (and proportionally large size of dataset), the point cloud has been split into 19427 files representing rectangular sections 720m by 480m. An accompanying shapefile allows a user to navigate to the files representing an area of interest, and additionally provides information about contractor, accuracy, survey date, project name and available products (DEM, DSM etc.).

Point cloud data used in this project is in LAZ format, which is an optimized compression of LAS format, and altogether takes about 324GB of disc space. Figure 5



Figure 4: Auckland Lidar 2016 survey capture extent

shows sample LAS file (AZ30\_3246\_2016), coloured by intensity, viewed in Displaz software, and information for the same tile, recorded in a shapefile.

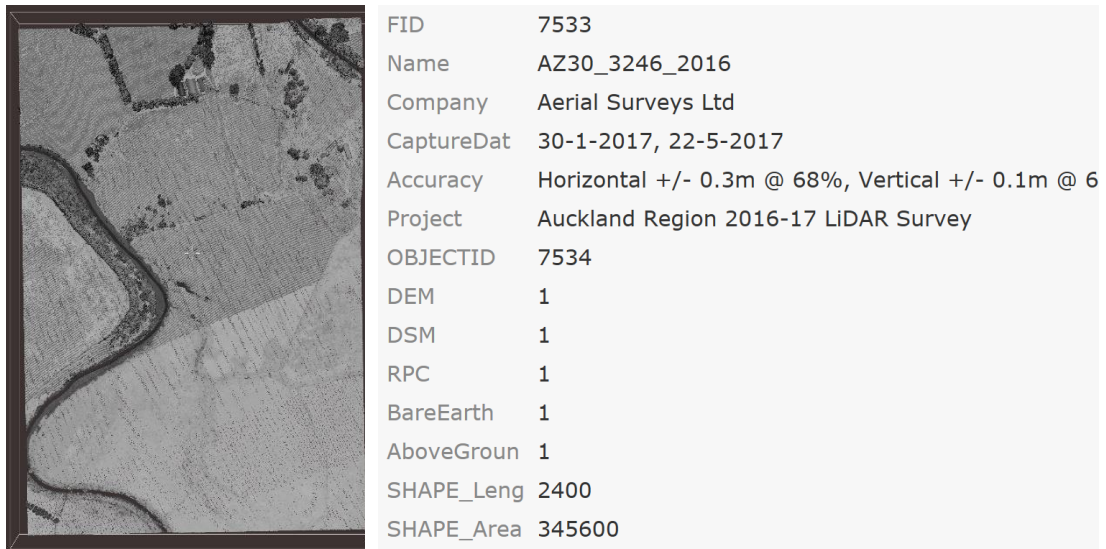


Figure 5: Sample LAZ file and corresponding tile information

## Point cloud data

LAS (and LAZ) is an open format designed specifically to handle point cloud data. It not only handles the information in a way to reduce file size, but also is a structured format that allows working with the data in a variety of software packages. In a LAS 1.2 file, each point comes with information recorded along with it. This available information includes: position (x,y,z), GPS time, intensity, return number, number of returns (for that specific emitted laser beam), point source ID (referring to a flight path ID), scan direction flag (referring to the direction of mirror movement), edge of flight line (allowing to distinguish last points recorded in a scan line, before mirror changes direction), scan angle (between -90 to 90, with 0 being nadir – directly below the aircraft), and classification (according to a key shown in Table 1, based on dataset metadata file and LAS1.2 specification). While the LAS 1.2 format allows also for recording colour in RGB format and additional user data, the Auckland 2016 Lidar dataset does not include this extra information. Nevertheless, recorded data allows for a wide range of analysis, such as comparing points from different flight paths, filtering based on number of returns, evaluating ground cover and more.

Originally, Auckland Lidar data comes in NZTM coordinates (EPSG:2193), but data used in this study has been projected to use the local datum – Mount Eden Circuit 2000 (EPSG:2105). Height values are presented using the Auckland Vertical Datum 1946.

Expected point cloud accuracy according to the data provider is 0.3m horizontal and 0.1m vertical (+/-0.1m at 68% confidence level). During the QA process it has been determined that most of the ground points are within 0.04m (for clear surfaces) from true vertical position, which makes the data much more usable for variety of purposes. Areas covered by vegetation have lower accuracy and some show significant errors. For this reason, this study will aim at determining overlapping factors (reoccurring point characteristics) of accuracy deterioration.

Table 1: Point cloud classes

| <b>Class</b> | <b>Represented feature</b>     |
|--------------|--------------------------------|
| <b>1</b>     | Unclassified                   |
| <b>2</b>     | Ground                         |
| <b>3</b>     | Low vegetation (0-0.3m)        |
| <b>4</b>     | Medium vegetation (0.3-2m)     |
| <b>5</b>     | High vegetation (2m and above) |
| <b>6</b>     | Buildings                      |
| <b>7</b>     | Noise                          |
| <b>8</b>     | Model key-point                |
| <b>9</b>     | Water                          |
| <b>10</b>    | Bridges                        |
| <b>11</b>    |                                |
| <b>12</b>    | Overlap                        |

### 3.2 Software

Multiple software packages have been used in this project. Some were used to process data and generate project results, while others were tools to analyse data visually. All of them are listed in appendix C.

### 3.3 Data Investigation

Significant research time has been devoted to exploring and examining the Lidar data. Apart from learning about the files structure and contents, as described in the “Study Area and Data” section, it was important to look at point clouds in different areas, as well as performing certain operations to get more insight of data availability and quality and to enable experiment planning.

#### Tiles: point source IDs, intensity values and classification

Below, as an example, tile BA31\_0437\_016 is examined. It is covering a rural area north of Auckland region, and the data has been collected on the 30/07/2017 and 19/10/2017. Recorded data is investigated using Displaz. Firstly, Figure 6 shows points symbolized by their classification. White noticeable straps are mostly an unclassified “overlap” (class 12) (but also class 1 – unclassified and 7 – noise). Apart from that, few classes are clearly visible: red buildings, shades of green – different vegetation classes and brown – ground. It is apparent that some areas have more dense low vegetation and possibly less penetration to the ground.

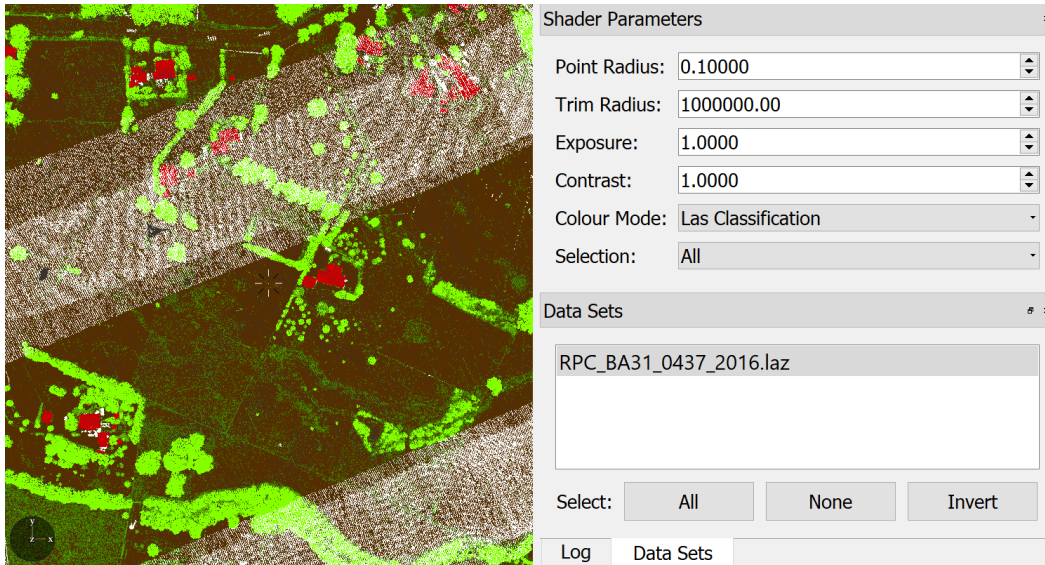


Figure 6: BA31\_0437\_2016: LAS Classification. Different shades of green represent points classified as vegetation; red is class 6 (buildings). White stripes are an unclassified overlap portion of the cloud.

The same data, but this time coloured by intensity, can be seen below on Figure 7. A clear pattern is visible – higher intensity points have been recorded on the northern part of the tile.

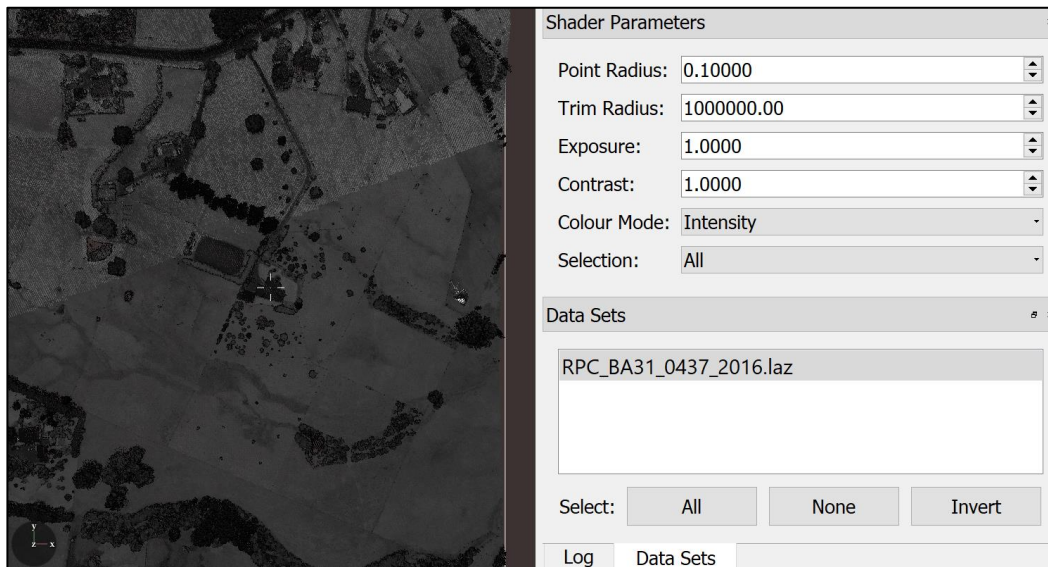


Figure 7: BA31\_0437\_2016: Intensity. Points of higher intensity are displayed in lighter shades of grey, points of lower intensity – in darker shades of grey.

When the points are displayed by their point source in Figure 8 (unique for each flight pass), a deduction can be made that the higher intensity points were specific to one of the flight passes. Intensity depends on a few different factors, such as surface type, moisture, or number of returns. Data for this tile has not been recorded all at once – in fact, there was an over two month period between different flight passes. Some data was recorded at the end of July, which is a middle of New Zealand’s winter. Another portion was surveyed in the second part of October – well into springtime.

Vegetation growth, and possibly different moisture levels could be the cause of different intensities.

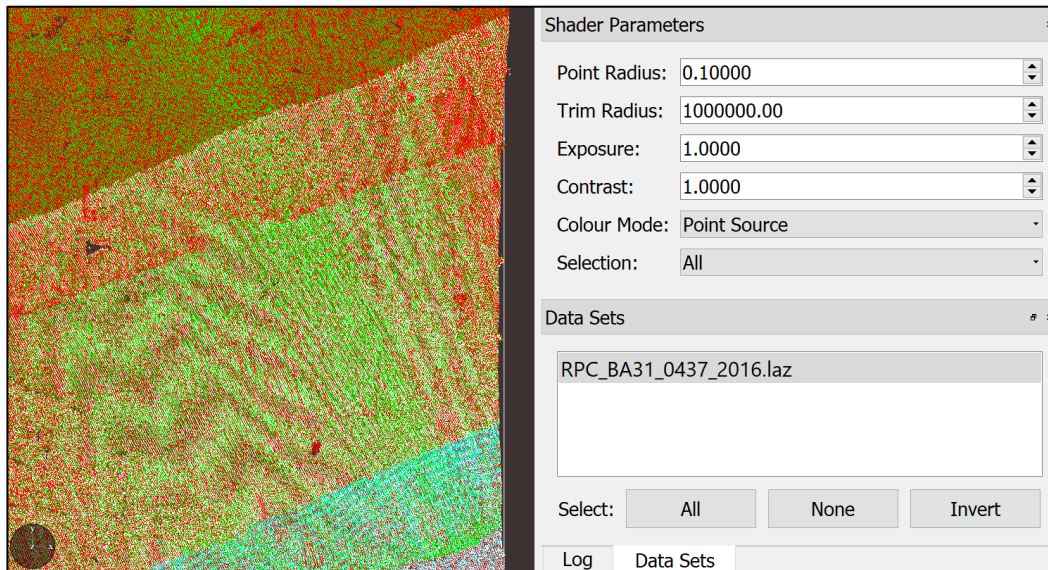


Figure 8: BA31\_0437\_2016: Point source. Points of different colours have been collected by different flight paths.

When investigating a thin slice of data, as pictured on Figures 9 and 10, it can be seen that the higher intensity points are aligned with lower intensity ones (Figure 10) and are classified in the same way (as ground) (Figure 9).

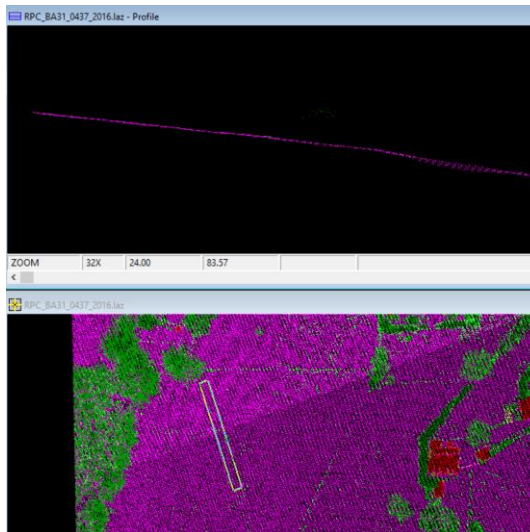


Figure 9: BA31\_0437\_2016 slice – class. Points classified as ground appear pink, vegetation shows in green and man-made structures in red. Lower part of the figure shows point cloud view from above, with narrow rectangle selecting a portion of the data to display in the top section of the figure – a profile view of the point cloud slice.

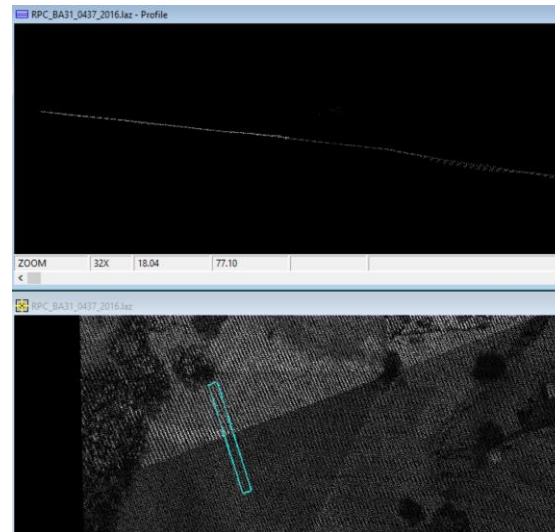


Figure 10: BA31\_0437\_2016 slice – intensity. Points recorded with higher intensity show brighter, closer to white, while low intensity points are darker shades of grey. Lower part of the figure shows point cloud view from above, with narrow rectangle selecting a portion of the data to display in the top section of the figure – a profile view of the point cloud slice.

No obvious issues have been noticed in case of tile BA31\_0437\_2016, but a different data sample, AZ30\_4745\_2016, shows possible data problems.

Figure 11 shows point cloud captured on the 23/11/2016 and 6/02/2017. When examining point intensity values (A), there is a clear pattern visible, where different flights recorded points of different intensity. This time however, higher intensity points do not align with the lower intensity ones (C). When symbolizing point cloud by classification (B and D) it can be seen that higher points are classified as low vegetation. One of the flights picked up more vegetation than the other (E), which can be due to a seasonal change. Figure (D) clearly shows that higher points have been classified as low vegetation. When symbology is applied by source ID -flight (E), it becomes apparent that one of the flights did not penetrate to the ground, and only picked up vegetation (blue points), while the other two flights present in the sliced area (red and orange) did not record any vegetation above the ground level.

It can be argued that there is nothing wrong here – one of the flights might have been completed when vegetation was taller, denser, and harder to penetrate – and achieving ground points was not possible. Overlapping flights picked up the ground height. However, the situation must be considered where all flights would not penetrate to the ground, or, where no overlapping data from different sources would be available – would it still be possible to determine that the recorded information was low vegetation and not ground (or would miss classification be possible)? Intensity clearly stands out as a differentiating factor between ground and vegetation here, but as shown in case of tile BA31\_0437\_2016, this is not necessarily a good indicator. Perhaps the roughness of points geometry is a better warning flag - points classified as vegetation do not form an equally smooth surface as the ground points on figures above. The problem is clearly visible, and the possible relationship between points characteristics and data quality is a focus of this paper.

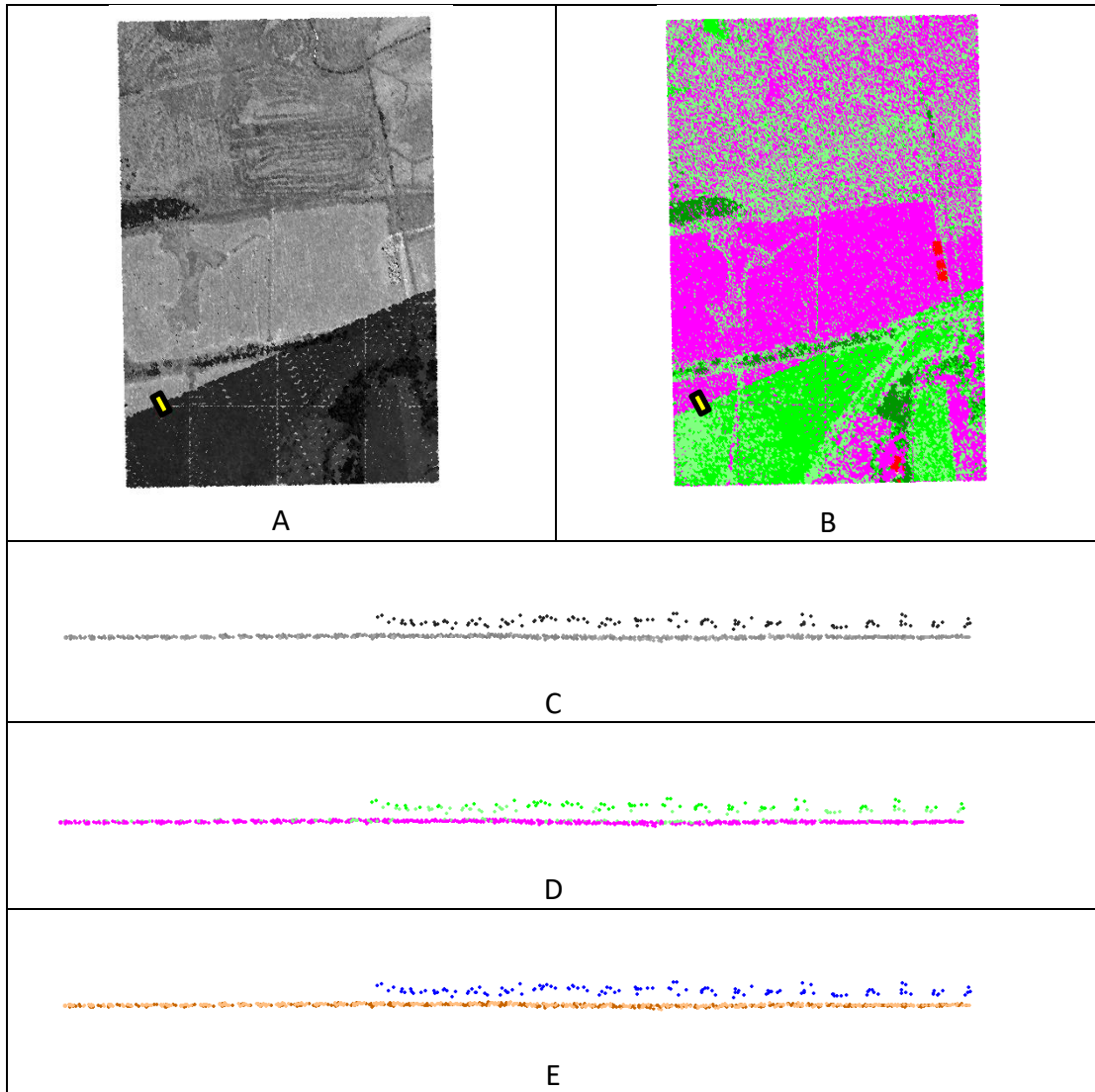


Figure 11: AZ30\_4745\_2016. A: View from above, points symbolised by intensity. Points recorded with higher intensity show brighter, closer to white, while low intensity points are darker shades of grey. Narrow yellow rectangle shows the cross-section location (C-E). B: View from above, points symbolised by classification. Points classified as ground appear pink, vegetation shows in green and man-made structures in red. Narrow yellow rectangle shows the cross-section location (C-E). C: Profile view, points symbolised by intensity. Lower intensity points visible above higher intensity points. D: Profile view, points symbolised by classification. Points above ground classified as low vegetation. E: Profile view, points symbolised by source ID (flight path). Lower points picked up by two flight paths, higher points picked up by a different flight path (with no penetration to the ground).

### 3.4 Data selection

As mentioned in previous sections, the dataset used in this study covers a vast area and is significant in size (over 300GB of data in compressed, storage efficient LAZ format). For a research project, this is a great advantage in terms of data availability across multiple areas with different characteristics, but poses an obvious problem of time-consuming computations, as well as large size interim datasets. Even the most efficient programs designed to deal with large data volumes, would not handle the whole available point cloud easily. Computation intensity aside, analysing data characteristics, on a large scale, also has proven to be difficult during work on this project. For this reason, 10 relatively small (ranging from 2.76ha to 42.95ha) test areas have been selected. All selected areas are covered by low vegetation but include both farmland and urban recreation areas (such as sport grounds and a golf course). Locations of the 10 areas can be seen on Figure 12.



Figure 12: Test areas locations



Figure 13 shows four examples of selected test areas.



Figure 13: Test areas examples

### 3.5 Data processing / manipulation

This section includes an overview of methods used in this project. An in-depth description of each step taken to obtain data for the analysis can be found in appendix D.

This thesis contains two different approaches used to obtain material for analysis.

The first and primary methodology used a computed difference between DEM values derived from different flight passes as a measure of accuracy that is examined against different derived point cloud characteristics. Digital elevation models used in this research have been created by interpolation: software uses point clouds to create a temporary triangulated irregular network (TIN), and extracts values of the TIN at cell centres. Methodology builds on a previous research ideas of accuracy relationship with incidence angle (scan angle and slope characteristics), and using intensity to help with classification and quality assessment (intensity characteristics). Furthermore, methodology extends further to examine other characteristics (presence of other class objects in the area, presence of other features within the laser path, roughness of point cloud). Accumulation of factors potentially linked to poorer quality or misclassification was expected to bring more robust accuracy deterioration detection.

The second methodology used points classified as ground and low vegetation and examined/compared derived point characteristics in these two classes. Accumulation of factors characteristic to one class and not the other, was expected to enhance misclassification detection.

#### Workflow overview

The first of the processes used to obtain results for analysis is pictured below on Figure 14. Summarised inputs and products are shown in dark rectangles. They are grouped by the software they are created with.

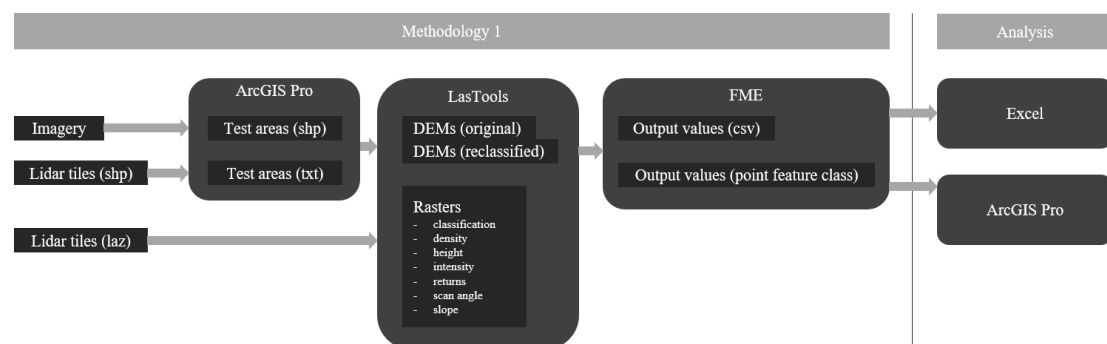


Figure 14: Methodology 1 overview chart

Second process, an addition analysis, is pictured below (Figure 15).

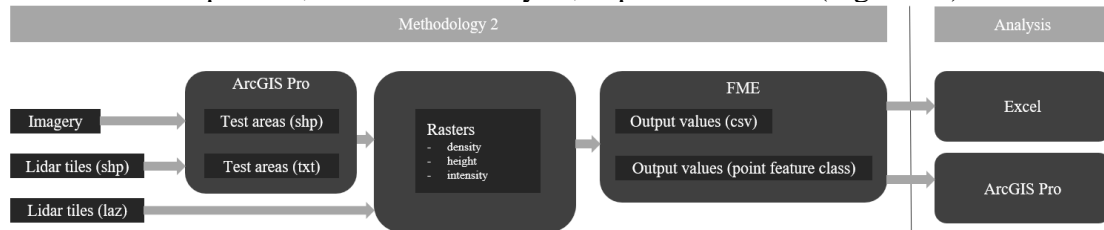


Figure 15: Methodology 2 overview chart

The initial inputs include Imagery (World Imagery service provided with ArcGIS Pro software as a base map), shapefile with Lidar tiles (extents and information) and point cloud (Lidar tiles, in laz format). Imagery is firstly used in ArcGIS Pro to create test areas polygons, and a Lidar tiles shapefile is used to intersect with these polygons and output a text document with relevant LAZ file directories. These two outputs, together with Lidar tiles (LAZ) (and subsequent products) are used as inputs in various batch file (BAT) scripts utilising LAStools. The final products of these scripts – various ASC files (elevation values and multiple data characteristics in raster form) are then written into CSV and a point feature class (to allow multiple attributes per cell/point) using FME software. The two types of outputs can then be analysed numerically and visually – in this project, using Microsoft Excel and ArcGIS Pro.

Input data (imagery, and Lidar data) is detailed in previous section (“Study Area and Data”). The processing of data is described briefly below. For further details, see appendix D.

#### Workflow – ArcGIS Pro

A shapefile with polygons around selected low vegetation areas has been created and used to extract a list of intersecting LAS files. For additional analysis (Methodology 2) a smaller subset has been used.

#### Workflow – LAStools

LAStools was the primary software used in this project. Most of the data manipulation has been conducted with script files using LAStools, and products for analysis have been partially created at this step. The chart (Figure 16) visualises the workflow from inputs (test areas list in text form, test areas shapefile and Lidar data in laz format) to intermediate products (ascii files) with use of batch files.

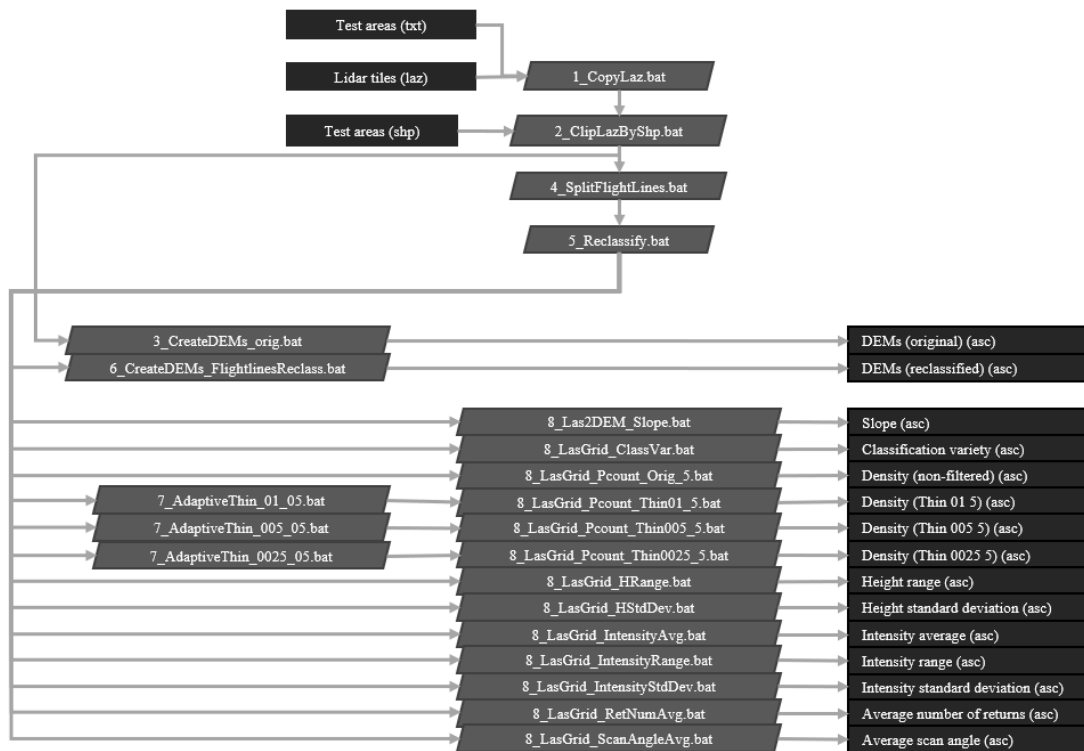


Figure 16: LAsTools workflow (Methodology1)

Additional processing as pictured in Figure 17, concentrated on a subset of areas analysed using first approach. No DEM discrepancy was needed for the second methodology, and the amount of studied characteristics has been cut down.

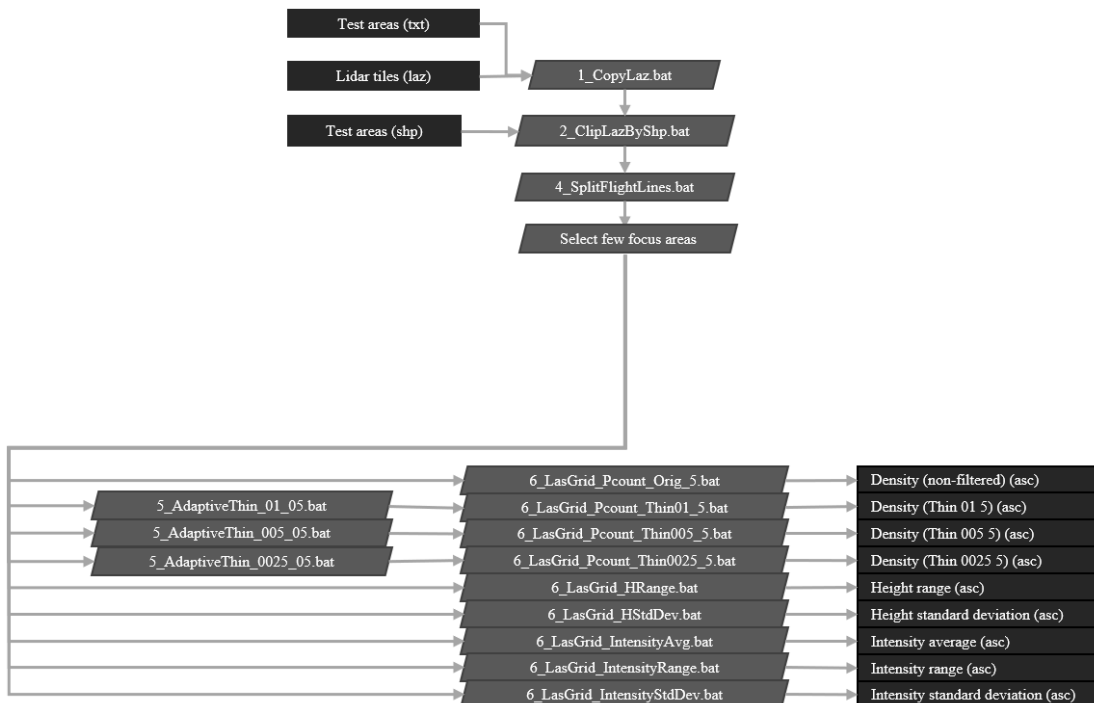


Figure 17: LAsTools workflow (Methodology 2)

A resolution of 5m has been selected for the products. While it may seem quite coarse, working with smaller volumes of data is easier (in terms of processing time,

storage capacity and results analysis). 5m resolution is enough to compute differences and spot possible relationships, especially when the examined data is collected over homogenous surfaces (low vegetation areas). For reasons of simplicity, it was better to use the same resolution for all products, and while some information might work better with more detailed resolution (such as intensity), other products required larger cell sizes (such as point counts). Taking all that into consideration, a resolution of 5m is a reasonably good choice. Studying data of this resolution can also allow us to spot interesting looking smaller areas and then examine them in more detail if required. The steps taken to produce these 5m resolution raster files are described in appendix D.

#### Workflow – FME

5m resolution raster datasets were created using LAStools, then were combined using FME to output as CSV file for analysis and point feature classes with multiple attributes. The process is summarized in appendix D.



## 4. Data analysis

As a result of the data manipulation described in the previous section, files enabling the analysis were created. This section outlines the contents and study description of these outputs. The possibility of the detection of low accuracy areas without the usage of additional products (such as ground control surveys) is evaluated in this part of the report.

### **4.1 Analysis of relationship between various Lidar point characteristics and the measure of accuracy: correlation and regression**

The primary product that was created to enable the analysis, and therefore examine the thesis objective, was a CSV file, relating various characteristics for each cell in a tabular form. The columns in the file are listed below:

- FileName\_core: name of the original Lidar tile that was the source of the data, with suffix indicating flight line/source ID.
- X and Y: indicating the coordinates of the centre of the cell
- DEM\_ref\_value: the value of the original DEM (before splitting flight lines and reclassifying the data)
- DEM\_value: the value of the DEM based on split flightlines, reclassified data
- DEM\_diff: the difference between the DEM\_ref and DEM\_value
- DEM\_abs\_diff: the absolute value of the DEM\_diff – the measure of accuracy used in this project

The remaining columns contain values obtained by inspecting/extracting various point characteristics as described in methodology section (and in appendix D):

- Class\_variety
- Density\_orig, Density\_01, Density\_005, Density\_0025
- Height\_Range, Height\_StdDev
- Intensity\_Range, Intensity\_StdDev
- RetNum\_Avg
- ScanAngle\_Avg
- Slope

The full CSV file consisted of 339795 rows of data, each representing a 5m by 5m wide cell with summarised characteristics. It is a reasonable data sample to use for the relationship analysis. Excel was used to compute statistics and therefore determine potential relationships and their strength.

### **Correlation**

The most common way to determine the existence and magnitude of similarity between variables is through the correlation coefficient. A strong positive relationship is visible when correlation coefficient values are close to 1, while a negative relationship produces values towards -1. Correlation values close to 0 are calculated for

variables that have weak to no relationship (variables appear to be independent of each other, one does not influence another). The correlation coefficient tests linear relationship between the variables.

Correlation coefficient has been computed between each tested characteristic and the DEM difference. The findings are outlined in the results section.

## Multiple regression

In multiple regression analysis, instead of trying to determine strength of relationships between different (individual) variables, all chosen (independent) variables are used as an input to finding a best-fit equation, that computes the dependent variable as closely as possible as a function of the independent variables. This analysis has been performed as the desirable outcome of this research was to find multiple characteristics that when present together, would flag possible data issues.

With this in mind, multiple regression has been used to study the combined relationship between the measure of accuracy and the different derived point cloud characteristics. The values have been computed using Excel. The findings can be seen in the results section.

### **4.2 Additional analysis**

A major cause of low data accuracy is a misclassification of point cloud. A second approach of data assessment focused on studying class 2 (ground) and class 3 (low vegetation) point cloud characteristics. Two separate CSV files are used in this additional analysis: one for each of the studied classes. Each file summarises the same characteristics derived for the 5m x 5m cells: original and filtered densities, height range and standard deviation, and intensity average, range, and standard deviation. Average values have been pulled out to spot any trends, and they can be seen in the graphs in results section.

Further analysis included using a density 0.05 filter (refer to “Adaptive thin and point count” section in appendix D: Detailed Methodology), because it shows larger differentiating potential than 0.1 filter (and identical to 0.025 filter), and standard deviation values for height and intensity (these differences are higher than ranges or averages if looking at percentage difference). These three derived characteristics have been summarised for the two classes in the Figure 24 in the Results section.



## 5. Results

### 5.1 Correlation

“Table 2: Correlation coefficient” shows the computed correlation coefficient values based on the exported sample data. Only correlation values between the absolute DEM difference (the measure of accuracy) and the different characteristics are shown below (relationships between different characteristics, although present, are omitted here).

Table 2: Correlation coefficient

|                   | DEM (absolute difference) |
|-------------------|---------------------------|
| DEM_abs_diff      | 1                         |
| Class_variety     | 0.23926                   |
| Density_orig      | -0.12393                  |
| Density_01        | 0.232303                  |
| Density_005       | 0.229077                  |
| Density_0025      | 0.229077                  |
| Height_Range      | 0.16291                   |
| Height_StdDev     | 0.178945                  |
| Intensity_Average | -0.00946                  |
| Intensity_Range   | -0.00846                  |
| Intensity_StdDev  | -0.00658                  |
| RetNum_Avg        | 0.05629                   |
| ScanAngle_Avg     | 0.103354                  |
| Slope             | 0.209059                  |

The computations do not show any significant linear relationships between the used measure of accuracy and the tested variables. A more in-depth interpretation of the results is summarised below.

The coefficient is especially close to 0 for all intensity related characteristics, showing that high, low, changeable, or consistent intensity cannot indicate possible accuracy issues – there is no visible link.

Scan angle, slope, height range and standard deviation are all related variables, that influence the incidence angle of a laser beam with the ground. Correlation values are low, even though the relationship is known. There are some reasons why these variables do not appear to be strongly correlated. Firstly, as proven in the previous research (as described in the literature review), the relationship exists between the accuracy and the incidence angle between the laser beam and the surface, and while that angle is influenced by terrain variability and the scanning angle, it has not been explicitly computed and analysed in this paper. Secondly, other factors may have a higher impact on accuracy, diluting the results. Lastly, analysed areas may not be sloping sharply enough to show the accuracy issues, and furthermore, this relationship is likely not linear, and therefore not ideal to capture with correlation coefficient.

Interestingly, the average number of returns shows very low correlation with the measure of accuracy, while class variety shows the highest correlation from all tested variables. This is somewhat contradictory – when a number of returns is higher than 1, it indicates a presence of other classes. Looking at the data, the average number of returns (for class 2 points only), was 1, sometimes 2, and very rarely a higher value. Lack of correlation indicates that if a laser beam penetrated through to the ground, the accuracy was not influenced or compromised. The class variability relationship with the accuracy measure, on the other hand, implies that possibly areas that have a range of ground covers, such as a mix of different vegetation and/or man-made structures, can result in lower accuracies. Nevertheless, as mentioned previously, this relationship does not appear to be significant.

Original density shows an insignificant negative relationship with the accuracy measure. This is not surprising: in open areas, point density should be fairly uniform before applying any thinning algorithms, and in vegetation covered areas, ground point density would be lower, and potentially easier to miss-classify – therefore slightly higher errors are expected when point density is lower, which is exactly what a low, but negative correlation coefficient pictures.

Density of filtered point clouds show some relationship with the measure of accuracy. The computed coefficients have almost double the magnitude of unfiltered density data, and are positive, indicating that the less points per cell, the higher the chances that the data does not have accuracy issues. This was expected, as smooth surfaces indicate more reliable measurements than rough, highly variable ones (where tall grass could have been wrongly classified as ground). Less thinning (preserving more detail: 0.05m and 0.025m) resulted in slightly less meaningful relationship with the measure of accuracy than a coarser algorithm (0.1m).

Out of the tested variables, class variety and density of points (after applying thinning filters) showed the strongest relationship with the accuracy measure (however, in both cases it was below 0.24). Below scatter plots show class variety (Figure 19) and filtered (0.1) point count (Figure 18) charted against the absolute DEM difference.

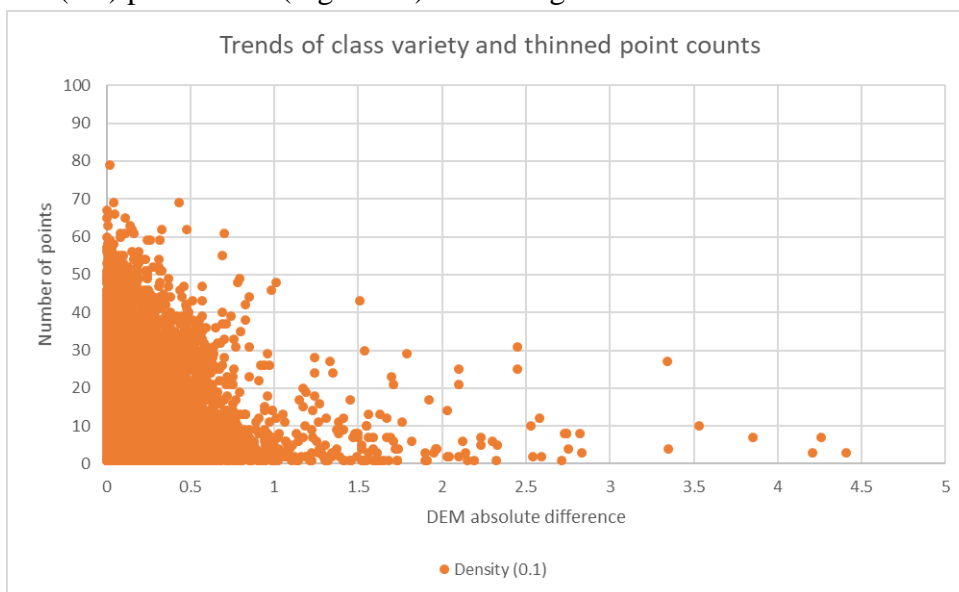


Figure 18: Scatter plot: Trends of thinned point counts. No clear relationship visible.

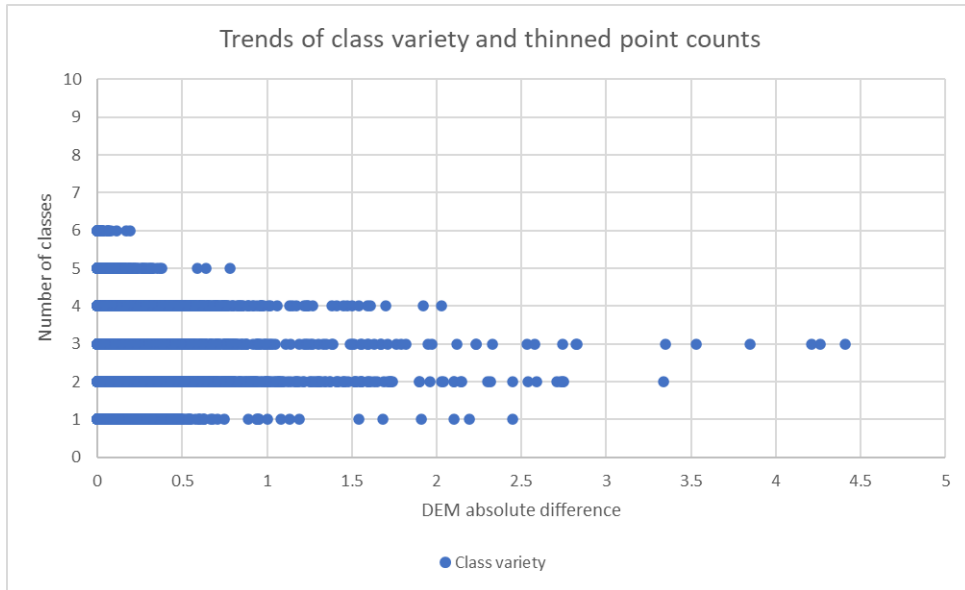


Figure 19: Scatter plot: Trends of class variety. No clear relationship visible.

Higher correlation values have been computed between some tested variables, as would be expected (for example, height range, height standard deviation and slope are all highly correlated, with values above 0.87). The relationship between class variety and density of thinned points was approximately 0.44 for the 0.1 thinning algorithm and 0.49 for the 0.05 or the 0.025 thinning algorithm, indicating that the correlation does exist, but is not very significant. The relationship between the class variety and the 0.1 thinned point count has been plotted and can be seen below (Figure 20).

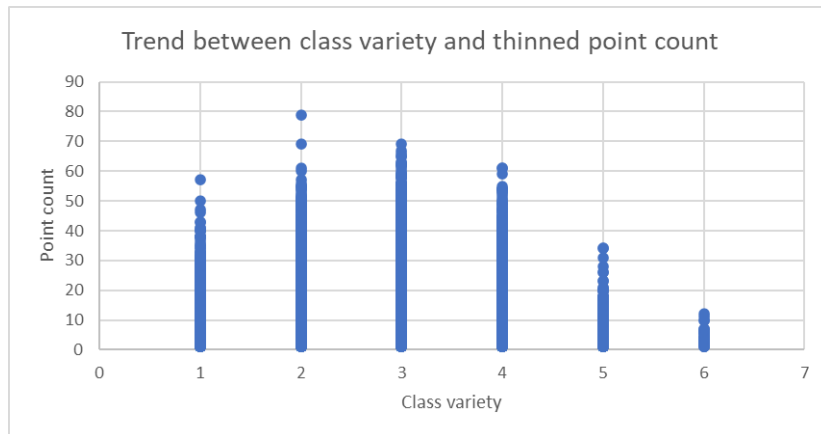


Figure 20: Scatter plot: Trend between class variety and thinned point count. No clear relationship visible.

The relatively weak relationship between these derived point cloud characteristics leads to a possibility that sometimes accuracy deterioration could be linked to one of these variables. Other times, it could be linked to another variable. There is a chance that when examining multiple variables simultaneously, the relationship (between a combination of variables and the accuracy deterioration) would be more meaningful.

## 5.2 Multiple regression

Table below contains results of multiple regression analysis.

Table 3: Multiple regression

SUMMARY OUTPUT

| Regression Statistics |             |
|-----------------------|-------------|
| Multiple R            | 0.344259767 |
| R Square              | 0.118514787 |
| Adjusted R Square     | 0.118480713 |
| Standard Error        | 0.075141501 |
| Observations          | 339794      |

| ANOVA      |        |             |             |             |                |
|------------|--------|-------------|-------------|-------------|----------------|
|            | df     | SS          | MS          | F           | Significance F |
| Regression | 13     | 257.9385982 | 19.84143063 | 3806.934057 | 0              |
| Residual   | 339781 | 1918.486843 | 0.005646245 |             |                |
| Total      | 339794 | 2176.425441 |             |             |                |

|                   | Coefficients | Standard Error | t Stat       | P-value     | Lower 95%    | Upper 95%    | Lower 95.0%  | Upper 95.0%  |
|-------------------|--------------|----------------|--------------|-------------|--------------|--------------|--------------|--------------|
| Intercept         | 0.003749248  | 0.000585651    | 6.401844162  | 1.5371E-10  | 0.002601389  | 0.004897108  | 0.002601389  | 0.004897108  |
| Class_variety     | 0.012532197  | 0.000180926    | 69.26715587  | 0           | 0.012177589  | 0.012886806  | 0.012177589  | 0.012886806  |
| Density_orig      | -0.00020525  | 2.54153E-06    | -80.75841412 | 0           | -0.000210231 | -0.000200268 | -0.000210231 | -0.000200268 |
| Density_01        | 0.000890347  | 5.41868E-05    | 16.43107236  | 1.20973E-60 | 0.000784143  | 0.000996552  | 0.000784143  | 0.000996552  |
| Density_005       | 0            | 0              | 65535        | #NUM!       | 0            | 0            | 0            | 0            |
| Density_0025      | 0.000728261  | 2.67313E-05    | 27.24379648  | #NUM!       | 0.000675869  | 0.000780654  | 0.000675869  | 0.000780654  |
| Height_Range      | -0.052522533 | 0.001345491    | -39.03594891 | 0           | -0.055159657 | -0.049885409 | -0.055159657 | -0.049885409 |
| Height_StdDev     | 0.103458902  | 0.005348716    | 19.34275473  | 2.60176E-83 | 0.092975574  | 0.11394223   | 0.092975574  | 0.11394223   |
| Intensity_Average | 2.91214E-07  | 6.7858E-08     | 4.291521507  | 1.77502E-05 | 1.58214E-07  | 4.24214E-07  | 1.58214E-07  | 4.24214E-07  |
| Intensity_Range   | -5.77802E-07 | 3.45007E-07    | -1.674756111 | 0.093983014 | -1.254E-06   | 9.8401E-08   | -1.254E-06   | 9.8401E-08   |
| Intensity_StdDev  | -2.07142E-06 | 1.31683E-06    | -1.573034273 | 0.115711814 | -4.65237E-06 | 5.0953E-07   | -4.65237E-06 | 5.0953E-07   |
| RetNum_Avg        | -0.006855813 | 0.000441447    | -15.53032647 | 2.25809E-54 | -0.007721036 | -0.00599059  | -0.007721036 | -0.00599059  |
| ScanAngle_Avg     | 0.001860766  | 2.53988E-05    | 73.26199139  | 0           | 0.001810985  | 0.001910547  | 0.001810985  | 0.001910547  |
| Slope             | 0.002726674  | 5.20487E-05    | 52.38699545  | 0           | 0.00262466   | 0.002828688  | 0.00262466   | 0.002828688  |

In this case, as noted before, correlation does exist between “independent” variables (there is a case of multicollinearity), and therefore multiple regression results can be unreliable. It is perhaps also worth mentioning that the coefficients shown in the bottom-most portion of the Table 2 are different to correlation coefficients computed in the previous section: the coefficient here is a multiplier of specific variable in the best-fit equation. It is partially related to a magnitude of influence on the dependent variable, however, it must be noted that different units of measure would affect (scale) this value (note low coefficients for intensity derived variables) hence, it cannot be deducted that the higher the value, the more influential it is on a final result, as was the case with the correlation coefficient.

The most meaningful value in the multiple regression analysis is the “R Square” value visible in the top section of Table 3. The multiple coefficient of determination,  $R^2$ , is a measure of percentage of variability in the dependent variable (absolute DEM difference), that can be explained by (computed with) the regression equation, and in this analysis it is approximately 0.1185. In other words, less than 12% of “low accuracy” can be explained using the regression equation. This is a very low value, proving that a combination of any of the tested variables cannot be used to determine possible Lidar accuracy problems.

### 5.3 Additional analysis

Average cell values for class 2 (ground) and class 3 (low vegetation) have been computed and can be seen in graphs below.

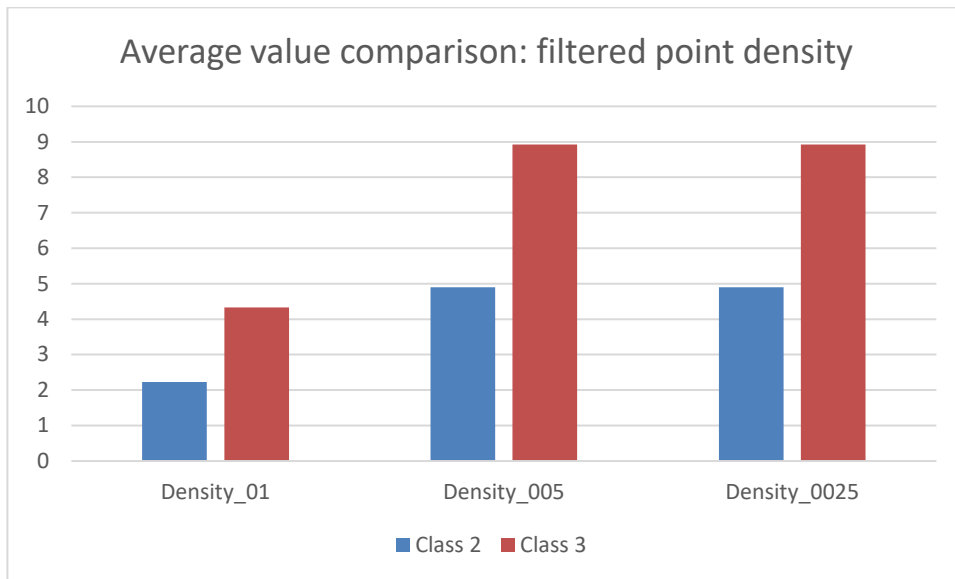


Figure 21: Additional analysis: average value comparison between class 2 (ground) and class 3 (low vegetation): filtered point density (with 0.1m, 0.05m and 0.025m filter tolerance)

On average, cells contained more points for low vegetation than for ground, after applying various size density filters (Figure 21).

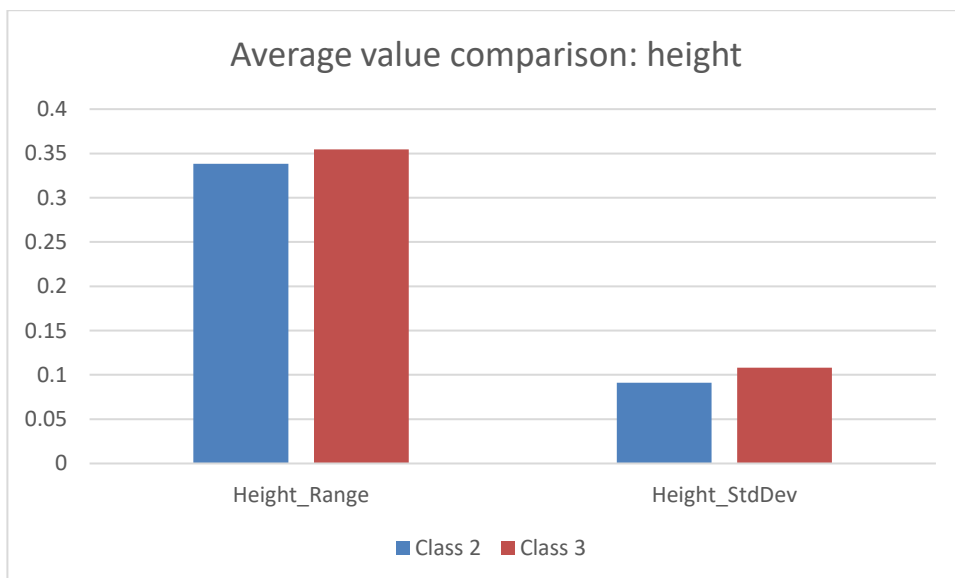


Figure 22: Additional analysis: average value comparison between class 2 (ground) and class 3 (low vegetation): height range and height standard deviation

On average, vegetation shows higher height range and standard deviation per cell (Figure 22).

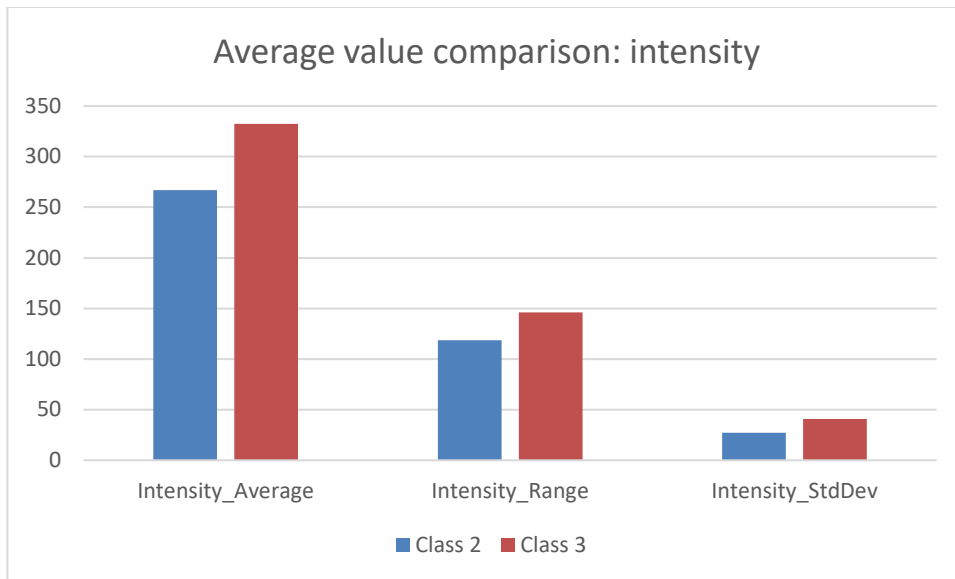


Figure 23: Additional analysis: average value comparison between class 2 (ground) and class 3 (low vegetation): average intensity, intensity range and intensity standard deviation

Ground points tend to have lower intensity, as well as less variable intensity within cells as compared to low vegetation (Figure 23).

Although some trends are apparent, it is not clear if specific values of these characteristics can point towards correct or wrong classification of Lidar points.

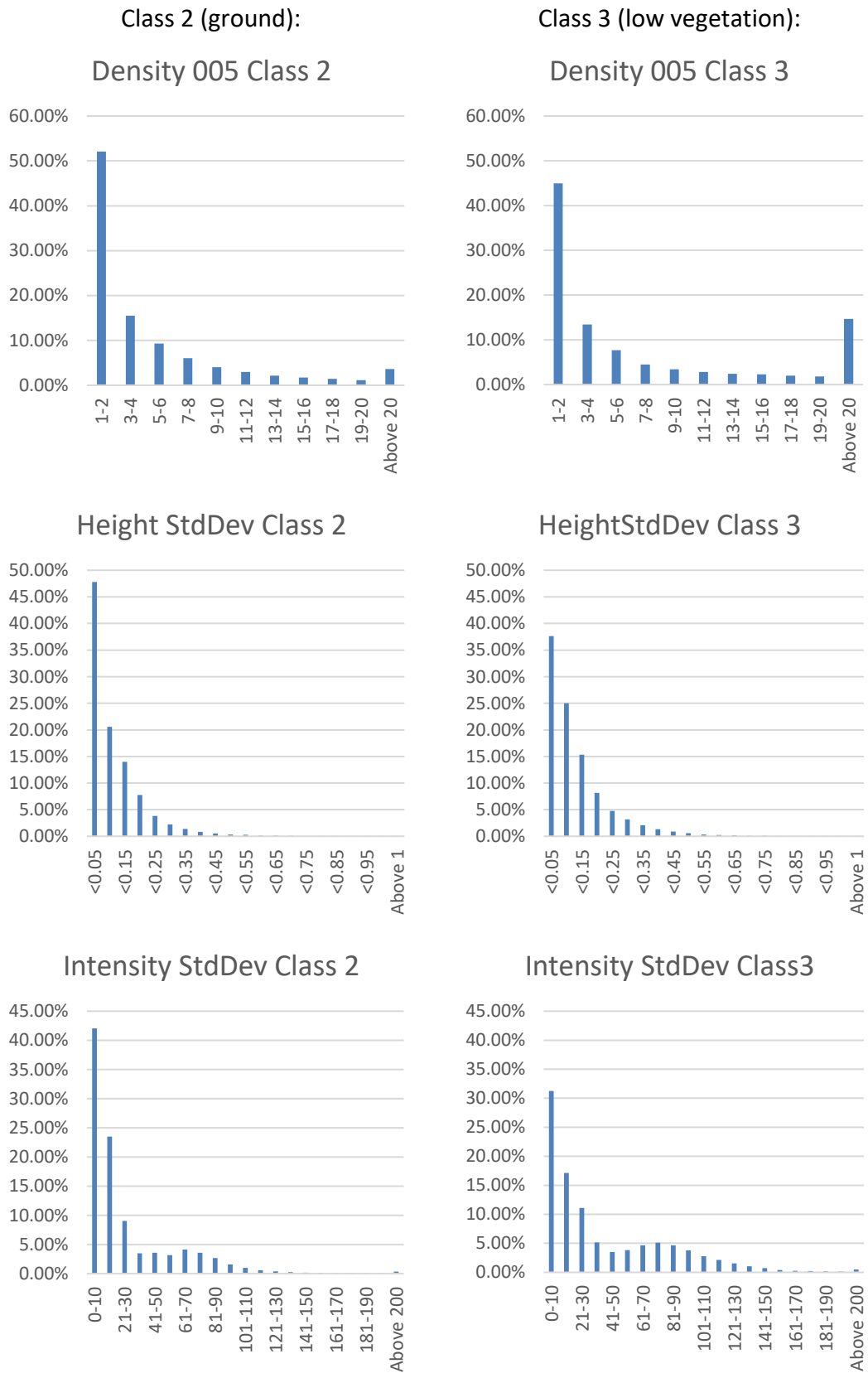


Figure 24: Class 2 (ground) and Class 3 (low vegetation) comparison. Each graph shows the percentage of cells falling within each threshold. For density filter tolerance 0.05, it shows what percentage of cells had 1-2 points, 3-4 points etc. For height, it shows what percentage of cells had a standard deviation of 0 to 0.05, 0.05 to 0.1 etc.

As may be seen on the histograms in Figure 24 above, in density comparison, more cells have been classified in all categories of 13 points and above for Class 3 than Class 2. There is no sharp cut-off value at which it could be deduced that the class 2 point may be misclassified, and in fact should belong to class 3, however, that probability rises with each extra point counted within a cell. Similarly, class 3, low vegetation, shows a consistently larger percentage of cells in higher categories of height standard deviation than class 2 – ground. The value is lower only in the lowest threshold: 0 to 0.05. Again, there is no identifiable cut-off point, and, in this case, the percentage of cells in higher categories decreases for both classes in a pattern not allowing us to draw any conclusions regarding the probability of misclassification. Intensity standard deviation comparison is slightly more promising in detecting classification issues. Low vegetation yields higher intensity standard deviations compared to the ground. 7.09% of class 3 cells had intensity standard deviation of above 110, while only 2.21% of class 2 cells fell in this category.



## 6. Discussion and conclusions

Work on this project included the manipulation of the point cloud (clipping point cloud portions, reclassifying data, extracting elevation information, summarising various point metadata), and exporting various information in tabular form to perform analysis in the form of statistical as well as graphical outputs.

The primary methodological focus was on the comparison of ground elevation obtained from the full dataset (assumed correct heights) and elevation obtained from reclassified point clouds originating from separated flight passes. Different point cloud characteristics (evaluated at 5mx5m cell level) were assessed against the discrepancy between the two elevation models.

Additional analysis included comparisons of point cloud characteristics between ground lidar points and low vegetation lidar points.

None of the computed correlation values were significant. Similarly, multiple regression analysis didn't detect any strong relationships between the tested lidar point cloud characteristics and the measure of accuracy. A comparison between class 2 and class 3 showed trends, however, no usable, specific values that could help with error detection could be derived.

The efforts described in this paper did not lead to developing a successful method for modelling areas within Auckland region that would have a potentially lower accuracy of Lidar data. If a stronger relationship between one (and ideally more) of the tested variables and the DEM absolute difference (the used measure of accuracy) would have been detected, further investigation could have been performed to fine-tune the testing and compute a meaningful regression equation. Then, analysis could be performed on larger areas or sites of interest (this time only extracting the independent variables needed as inputs to a regression equation). Zones of computed possibly lower accuracy could have been determined and visualized on a map or exported (for example as shapefiles) for future reference. Unfortunately, as described in the results section above, no meaningful relationships have been detected.

### 6.1 Research shortcomings

There are few reasons why no constructive results came out of this project. One obvious rationale could be that the low accuracy cannot be simply modelled using this available point cloud (and its metadata). This is most likely at least partially true: Even if results would be more promising, still only a percentage of low accuracy areas could be computed using this type of modelling.

Another reason for a failure of this experiment is that it had some flaws. First and foremost, the accuracy measure is far from ideal. In any other research paper tackling Lidar accuracy, a reliable survey information dataset has been used to determine the point cloud height correctness. This type of data has not been available, certainly not for large areas that have been analysed. For that reason, a discrepancy between digital elevation models computed from individual flight passes and the DEM values based on combined data was used, as described. Obviously, this is not ideal, as

a combined flights DEM is used here as the “true” height value, which would not always be the case. This has certainly been a trade-off: being able to work with large volumes of Lidar data across different low vegetation covered areas, but without a reliable enough accuracy measure. It is my belief that this crucial component of the thesis research design is the biggest problem in my methodology.

It is, however, not the only problem. There are some other considerations. One of them are different settings that could have been used in the computing functions executed with LAStools, especially the cell size used to analyse the data. It has been explained in the methodology section, why a cell size of 5m by 5m has been used (the resulting simplicity of the experiment being one of the bigger factors). When exploring the outputs of combined numerical values, however, it can be seen that this was likely not an ideal approach for some of the tested variables, and more meaningful values could have been extracted if a different cell size was used. If continuing research along these lines is conducted in a similar manner, my recommendation would be to differentiate cell sizes for different variables and use a procedure that would overlay the different size outputs instead.

Another approach that could be examined is a possibility of treating the accuracy as a binary measure (either acceptable or not), instead of as a continuous spectrum. It could have been interesting to see if any relationships would emerge in that scenario. Different statistical testing would have to be considered in such case.

Furthermore, it deserves restatement, that a proven, existing relationship between the accuracy and the incidence angle of the laser pulse, has not been properly treated in this research. The methodology developed as described in “Accuracy estimation for laser point cloud including scanning geometry” (Schaer et al., 2007) could have been incorporated to produce better results (however, in the absence of any other potentially meaningful variables, it is not needed).

Finally, the analysis of the results that has been described in this paper is problematic. Firstly, computing correlation has been used to spot any significant relationships between the tested variables and the measure of accuracy. Then, multiple regression has been used to see if a meaningful relationship exists when combining the variables. As stated previously, when initially investigating the topic, and designing the thesis work, it was hoped that some relationships would be discovered with correlation computations, and that multiple regression could then lead to obtaining a formula for flagging possibly lower accuracy Lidar data. This has certainly not happened, and a final possible reason for that is the non-linearity of the relationships between the tested variables and the measure of accuracy. Both: correlation and multiple regression, assume (and test) linear relationships. However, it is indeed possible that existing relationships (if any) could be non-linear, but instead follow different patterns (for example exponential).

## **6.2 Further research**

The idea of combining different variables, that each individually show relationship with accuracy, to determine with more confidence if portions of data have reliable, high quality, has its merits. Previous research (as well as simply understanding

Lidar technology and geometry principles) has indicated that the relationship between incidence angle and accuracy does exist. If any other variable is proven to show similar relationship, there is potential to revisit the methodology proposed in this paper.

One of the variables not tested in this paper, due to the lack of availability, was the thickness of the waveform part forming the detected peak (and resulting in point record).

In “Exploring the potential of full waveform airborne Lidar features and its fusion with RGB image in classification of a sparsely forested area” (Babadi M., Sattari M., Pour S. I.) the authors explore more precise vegetation classification from the point cloud, using waveform shape information – pulse characteristics. The paper also refers to multiple studies where point characteristics such as intensity and pulse width were used in classification of different vegetation species (as opposed to relying mostly on geometry of a point cloud). These pulse characteristics, unavailable for my study, could be used as additional test parameters.

Furthermore, a future study could include data from different Lidar system types. “A Photon-Counting Full-Waveform Lidar” (Du B.-C., Li Z.-H., Shen G.-Y., Zheng T.-X., Zhang H.-Y., Yang L., Wu G.) describes a system that records the number of photons returned to the instrument in a number of very small-time intervals, therefore mapping a waveform. This way, the obtained information (such as waveform peak and waveform width) about each recorded point is easier to quantify. It is somewhat a hybrid between the linear-mode full-waveform and photon-counting discrete-point systems. The authors write that: “The complexity of the waveforms is greatly reduced with short laser pulses, which facilitates the extraction of the signal pulse information. By virtue of the echo full-waveforms, more parameters of the scattering surface can be analyzed than in a traditional discrete-point Lidar, such as the vertical structure, peak position, peak amplitude, peak width and backscatter cross section, which are utilized to characterize the surface features of the targets for classification.” In the described test study, it is shown, for example, that peak width can help with detecting sloping surfaces. As it is known that incidence angle affects the recorded point accuracy, peak width recorded against the point could potentially signal (a portion of) discrepancy between the true and measured location. Other recorded pulse quantities could also be used in a similar study to the one described in this thesis, to check for possible relationship with accuracy.

### **6.3 Final word**

During work on this paper, a method for modelling low data quality has not been determined. There is certainly space for further investigations and/or improvement, as described in previous sections. For now, when using available Lidar data in applications requiring high accuracy elevation information, extra care must be taken. Firstly, point clouds covering the area of interest should be visually inspected. Secondly, data can be compared with older Lidar fly overs. If there is an inconsistency between different datasets, it should be evaluated if an expected change over time has occurred, based on available aerial imagery or possibly other data and local knowledge. Finally, a high precision terrestrial survey (of sample of the area of interest) may be

needed, to ensure Lidar data accuracy meets the requirements and can be used in a specific case.

## 7. References

Babadi M., Sattari M., Pour S. I. 2019. Exploring the potential of full waveform airborne lidar features and its fusion with RGB image in classification of a sparsely forested area. *The International Archives of the Photogrammetry, Remote Sensing and Spatial Information Sciences*, Volume XLII-4/W18, 2019.

Du B.-C., Li Z.-H., Shen G.-Y., Zheng T.-X., Zhang H.-Y., Yang L., Wu G. 2019. A Photon-Counting Full-Waveform Lidar. *Chinese Phys. Lett.* 36 094201.

ASPRS Accuracy Standards for Digital Geospatial Data. *Photogrammetric Engineering & Remote Sensing*. December 2013.

ASPRS Positional Accuracy Standards for Digital Geospatial Data. (Edition 1, Version 1.0. – November, 2014). *Photogrammetric Engineering & Remote Sensing*. Vol. 81, No. 3, March 2015. 0099-1112/15/813–A1.

ASPRS Guidelines Vertical Accuracy Reporting for Lidar Data V1.0. May 24, 2004.

Aguilar F.J., Mills J.P., Delgado J., Aguilar M.A., Negreiros J.G., and Pérez J.L. 2009. Modelling vertical error in LiDAR-derived digital elevation models. *ISPRS Journal of Photogrammetry and Remote Sensing* 65 (2010) 103-110.

Hubacek M., Kovarik V., and Kratochvil V. 2016. Analysis of influence of terrain relief roughness on DEM accuracy generated from LiDAR in the Czech Republic territory. *The International Archives of the Photogrammetry, Remote Sensing and Spatial Information Sciences*, Volume XLI-B4, 2016. XXIII ISPRS Congress, 12–19 July 2016, Prague, Czech Republic

Jordan, D., and Popescu, G. 2015. The accuracy of LiDAR measurements for the different land cover categories. *Scientific Papers. Series E. Land Reclamation, Earth Observation & Surveying, Environmental Engineering*. Vol. IV, 2015. Print ISSN 2285-6064, CD-ROM ISSN 2285-6072, Online ISSN 2393-5138, ISSN-L 2285-6064  
Mallet C., and Bretar F. Full-waveform topographic lidar: State-of-the-art. 2008. *ISPRS Journal of Photogrammetry and Remote Sensing* 64 (2009) 1-16.

ALS Point Cloud Format.

[https://www.usna.edu/Users/oceano/pguth/md\\_help/html/las\\_format.htm](https://www.usna.edu/Users/oceano/pguth/md_help/html/las_format.htm). Accessed 20/06/2021

Raber G.T., Jensen J.R., Schill S.R., and Schuckman K. 2002. Creation of Digital Terrain Models Using an Adaptive Lidar Vegetation Point Removal Process. *Photogrammetric Engineering & Remote Sensing* Vol. 68, No. 12, December 2002, pp.

1307-1315. 0099-11 12/02/6812-1307 2002 American Society for Photogrammetry and Remote Sensing.

Scaioni M., Höfle B., Baungarten Kersting A.P., Barazzetti L., Previtali M., Wujanz D. 2018. Methods from information extraction from LIDAR intensity data and multispectral LIDAR technology. The International Archives of the Photogrammetry, Remote Sensing and Spatial Information Sciences, Volume XLII-3, 2018

ISPRS TC III Mid-term Symposium “Developments, Technologies and Applications in Remote Sensing”, 7–10 May, Beijing, China.

Schaer P., Skaloud J., Landtwinig S., Legat K. 2007. Accuracy estimation for laser point cloud including scanning geometry. The International Archives of the Photogrammetry, Remote Sensing and Spatial Information Science, Vol. 36. Issue 5., 2007.

Regression analysis with Excel. <https://stattrek.com/multiple-regression/excel.aspx#:~:text=Regression%20Analysis%20With%20Excel,application%20that%20supports%20multiple%20regression.> Accessed 17/07/2020

Kirby, J. Cartographic Statistics 181. 2009 Edition. Course Manual. Curtin University of Technology, Faculty of Science and Engineering, Department of Spatial Sciences.

## **Appendix A**

Lidar 2016/2017 information (extracted from original text file):

This digital mapping dataset was created from airborne LiDAR sensor data collected 2016-17. The date that the data was collected is documented in the tile layout shapefile that accompanies the datasets.

The Point Cloud data is in LAS v1.2 and ESRI 3D point shape file formats. The LAS files contain classes 1- Unclassified, 2 - Ground, 3 - Low vegetation (0 – 0.3m), 4 - Medium vegetation (0.3 – 2m), 5 - High vegetation 2m > , 6 – Buildings, 9 - Water, 10 Bridges . Data is stored in LINZ Topo50 1k tiles (720m x 480m). Raw Point Cloud density is at least 4 points per square metre over open ground. Vertical accuracy is +/-0.1m @ 68% confidence. Point cloud heights are recorded in the Auckland 1946 NZVD2016 and NZVD2016 datums. Coordinates are NZTM. Coastal and intertidal data was collected at one and one half hours either side of low tide.

As part of the contract deliverables a final report will be prepared at the time of acceptance of the last data delivery that details the procedures followed in the creation of this dataset and which documents the results of point cloud accuracy checks.

The Airborne Global Position System (AGPS), inertial measurement unit (IMU), and raw scans are collected during the LiDAR aerial survey. The AGPS monitors the xyz position of the sensor and the IMU monitors the orientation of the aircraft. During the aerial survey laser pulses reflected from features on the surface and are detected by the receiver optics and collected by the data logger. GPS locations are based on data collected by receivers on the aircraft and base stations on the ground. The AGPS, IMU, and raw scans are integrated using proprietary software developed by Optech the and delivered with the Optech LiDAR System. The resultant file is in a LAS binary file format. The LAS file version 1.2 format can be easily transferred from one file format to another. It is a binary file format that maintains information specific to the LiDAR data (return#, intensity value, xyz, etc.). The unedited data are classified to facilitate the application of the appropriate feature extraction filters. A combination of proprietary filters is applied as appropriate for the production of bare-earth digital elevation models (DEMs). Interactive editing methods are applied to those areas where it is inappropriate or impossible to use the feature extraction filters, based upon the design criteria and/or limitations of the relevant filters. These same feature extraction filters are used to produce elevation height surfaces.

Filtered and edited data are subjected to rigorous QA/QC according to the agreed quality control plan and procedures. Very briefly, a series of quantitative and visual procedures are employed to validate the accuracy and consistency of the filtered and edited data. Ground control is established by registered surveyors. A suitable number of points are selected for calculation of a statistically significant accuracy assessment.

Accuracy validation and evaluation is accomplished using proprietary software to apply relevant statistical routines for calculation of Root Mean Square Error (RMSE).

#### NEDF Metadata

Acquisition Start Date: 01 November 2016  
Acquisition End Date: 29 June 2017  
Sensor: LiDAR  
Device Name: Optech  
Flying Height (AGL): 1650  
INS/IMU Used: Applanix  
Number of Runs: UNK  
Number of Cross Runs: UNK  
Swath Width: UNK  
Flight Direction: UNK  
Swath (side) Overlap: UNK  
Horizontal Datum: NZGD2000  
Vertical Datum: AUK46  
Map Projection: NZTM  
Description of Aerotriangulation Process Used: NA  
Description of Rectification Process Used: NA  
Spatial Accuracy Horizontal: 0.3  
Spatial Accuracy Vertical: 0.1  
Average Point Spacing (per/sqm): 4  
Laser Return Types: 4 pulses (1st 2nd 3rd 4th and intensity)  
Data Thinning: 1  
Laser Footprint Size: 0.3  
Calibration certification (Manufacturer/Cert. Company): NA  
Limitations of the Data: NA  
Surface Type: DEM  
Product Type: Points  
Classification Type: Level 1  
Grid Resolution: 1  
Distribution Format: LAS  
Processing/Derivation Lineage: NA  
WMS: NA?



## Appendix B



### **GEOSPATIAL DATA LICENCE AGREEMENT (CC BY International 4.0)**

**Legal Notice:** By accessing the material referred to below ("Material") (regardless of delivery method), you agree to the following terms. All copyright in the Material is owned by or licensed to Auckland Council. You may use, copy and adapt the Material in accordance with the Creative Commons Attribution 4.0 International licence, which can be viewed here: <https://creativecommons.org/licenses/by/4.0/legalcode>

Notwithstanding anything to the contrary, except as required by law, all Material is provided on an "as is" basis, without any warranty or representation of any kind (express or implied). Accessing, downloading and use of the Material is done entirely at your own risk and the accuracy of the Material should be independently verified before it is relied upon. Data representing Marine and Intertidal areas should not replace published navigation charts.

To the extent possible under law, Auckland Council will not be liable on any legal basis (without limitation, including negligence) for any direct, indirect or consequential loss or damage arising in connection with the Material to you or any third party. You will ensure that any parties that you provide the Material to are aware of these terms.

The following material is being licensed to you:

#### **2016 LiDAR Data**

##### **Formats available:**

- Raw Point Clouds
- Ground/Digital Terrain Model (DTM) Point Clouds
- Above Ground Point Clouds
- Digital Elevation Model (DEM)
- Digital Surface Model (DSM)
- Contours
- Imagery

## Appendix C

Software used in Master Thesis “ALS (AIRBORNE LIDAR) ACCURACY: CAN POTENTIAL LOW DATA QUALITY OF GROUND POINTS BE MODELLED/DETECTED? CASE STUDY OF 2016 LIDAR CAPTURE OVER AUCKLAND, NEW ZEALAND.”

### Displaz

Displaz is a software designed to visualize point cloud data. It enables user to view multiple laz/las files in the same time, display points by their characteristics (such as class or point source ID), query points x,y,z locations, zoom, rotate and limit view by radius from chosen point. Moreover, the software allows user to interactively customize visualizations by accessing part of software’s code (this functionality has been used for Figure 2 (Point cloud and recorded point properties, thesis background section). Although the only software’s ability is viewing point cloud files, it is a powerful tool for inspecting data. More information about Displaz can be accessed through a github page: <https://github.com/c42f/displaz>.

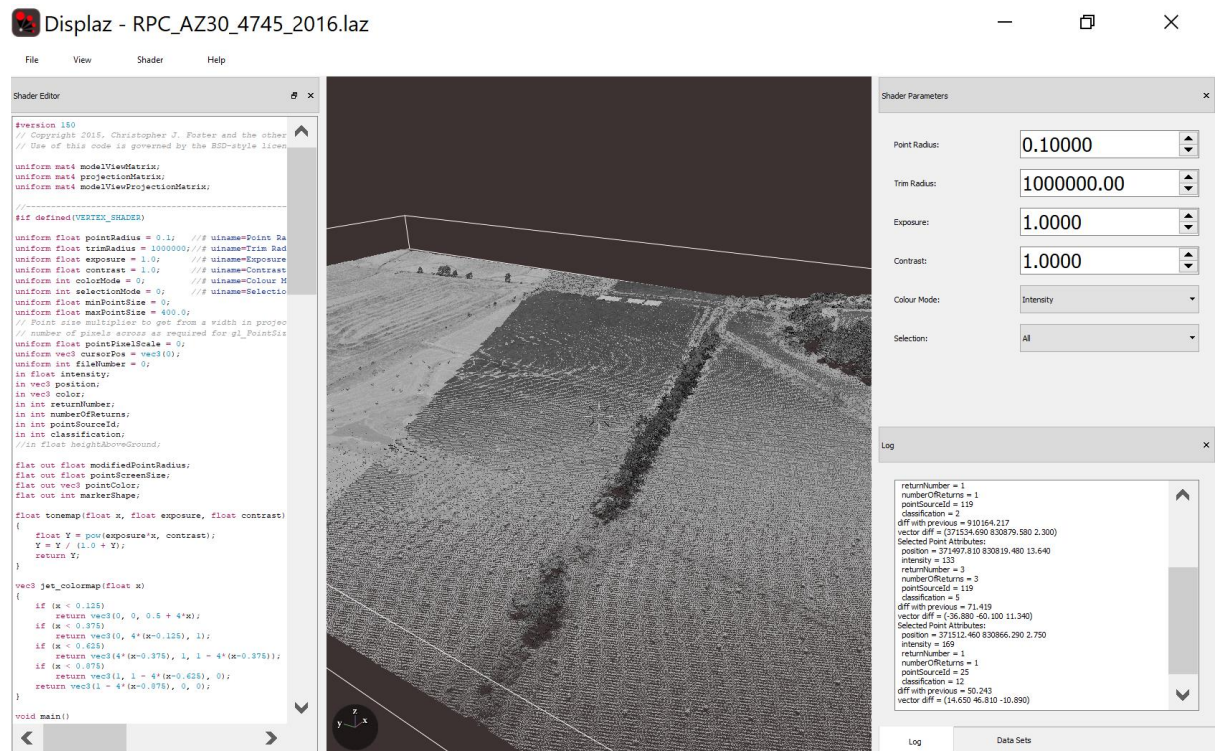


Figure 25: Displaz

### FugroViewer

FugroViewer is another software designed for visualizing point cloud data. Apart from symbolizing points by chosen by the user attribute, it has few more advanced options, such as overlaying points over a reference imagery, visualizing TIN and contours, inspecting points in different views (top down, side, 3D) and investigating sliced data (narrow long portion of point cloud). That last function is the main reason the software was useful in interrogating the data. More about this software package can be found on <https://www.fugro.com/about-fugro/our-expertise/technology/fugroviewer>.

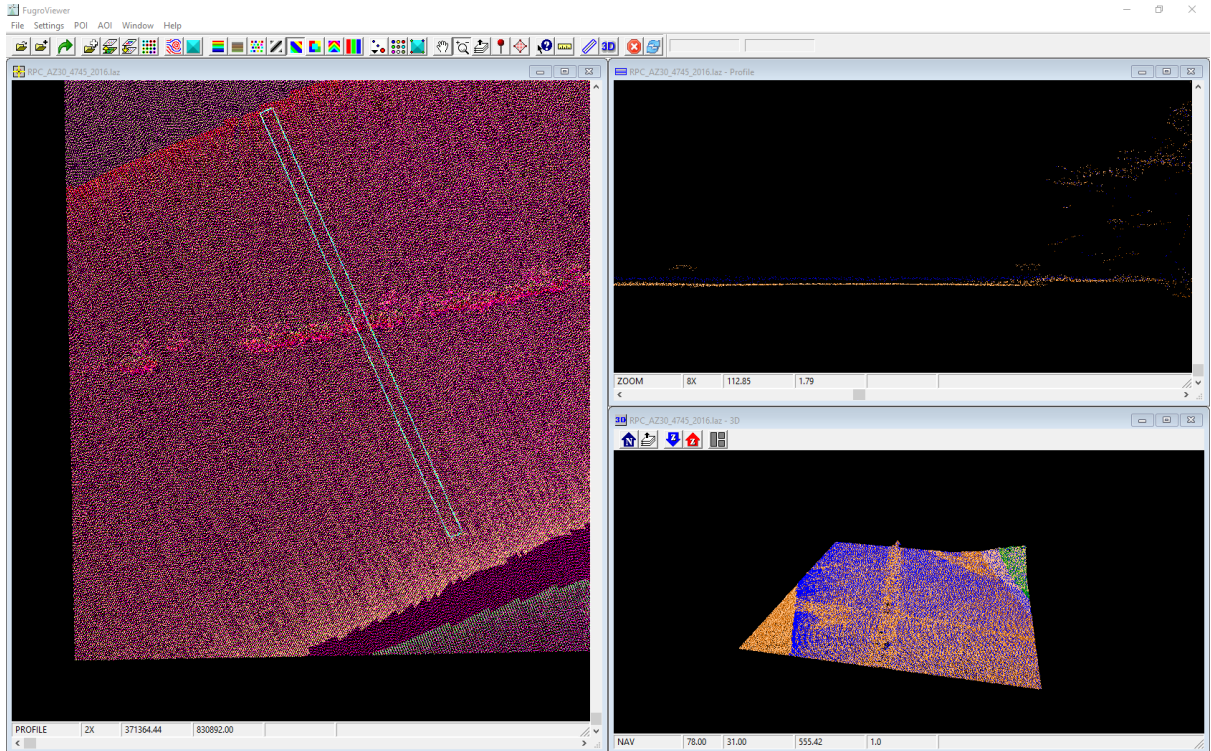
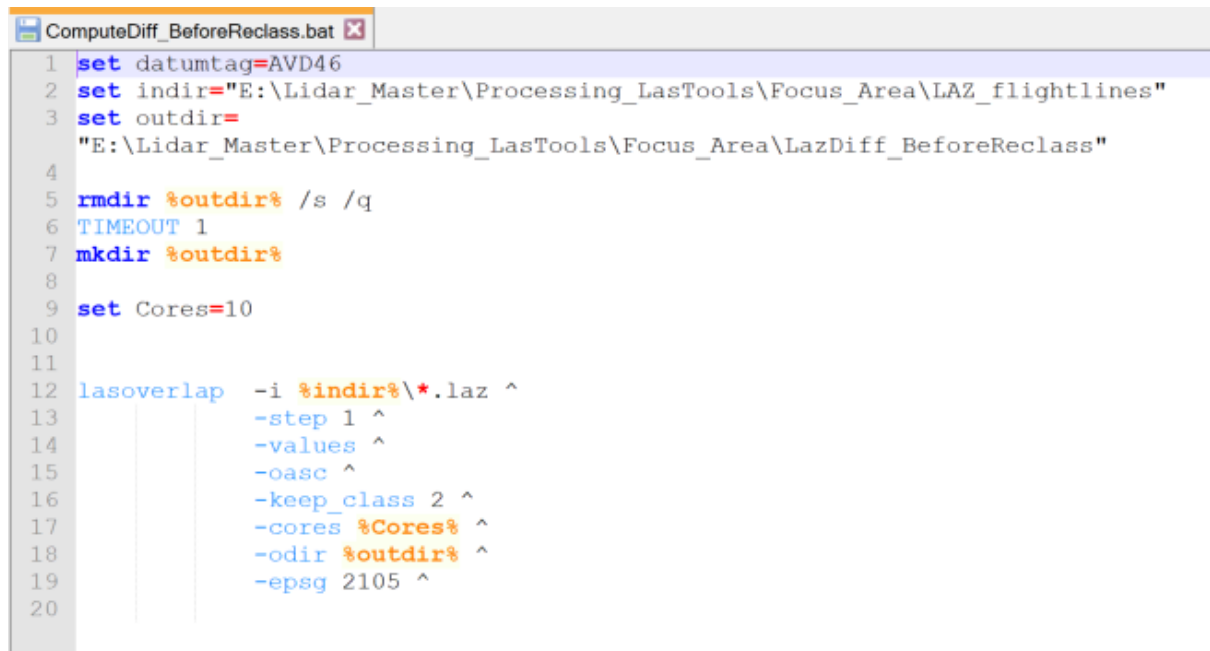


Figure 26: FugroViewer

## LAStools

LAStools is a software suite designed to process point cloud data. This highly efficient software is ideal for working with large datasets that can consist of millions of points. LAStools can be executed through a native program with user interface, as toolboxes that can be added to other software packages, such as ESRI's ArcGIS Pro, or as commands in scripts. Extensive documentation (in text file format) is available for every available command, with multiple examples of usage. In this project, LAStools have been executed through batch files, which gives the user most flexibility and enables processing of multiple files at once. More information on LAStools can be found on website: <https://rapidlasso.com/lastools/>.



```
1 set datumtag=AVD46
2 set indir="E:\Lidar_Master\Processing_LasTools\Focus_Area\LAZ_flightlines"
3 set outdir=
  "E:\Lidar_Master\Processing_LasTools\Focus_Area\LazDiff_BeforeReclass"
4
5 rmdir %outdir% /s /q
6 TIMEOUT 1
7 mkdir %outdir%
8
9 set Cores=10
10
11
12 lasoverlap -i %indir%\*.laz ^
13            -step 1 ^
14            -values ^
15            -oasc ^
16            -keep_class 2 ^
17            -cores %Cores% ^
18            -odir %outdir% ^
19            -epsg 2105 ^
20
```

Figure 27: example bat file executing LAStools - "lasoverlap"

## Notepad ++

Notepad++ is a text editor, that has been used to write batch files executing LAStools. <https://notepad-plus-plus.org/>.

## Windows PowerShell

Windows PowerShell is a Windows application (<https://docs.microsoft.com/en-us/powershell/>) and has been used in this project to execute LAStools through bat files (while bat files can be executed just by double clicking them, executing them through Windows PowerShell allowed trouble-shooting on some occasions).

## FME

FME (Feature Manipulation Engine) is a software package distributed by Safe Software. FME can work with a rich variety of formats and allows users to create simple to complex data manipulation workflows consisting of connected transformers. More information about FME can be accessed through Safe's site: <https://www.safe.com/fme/>.

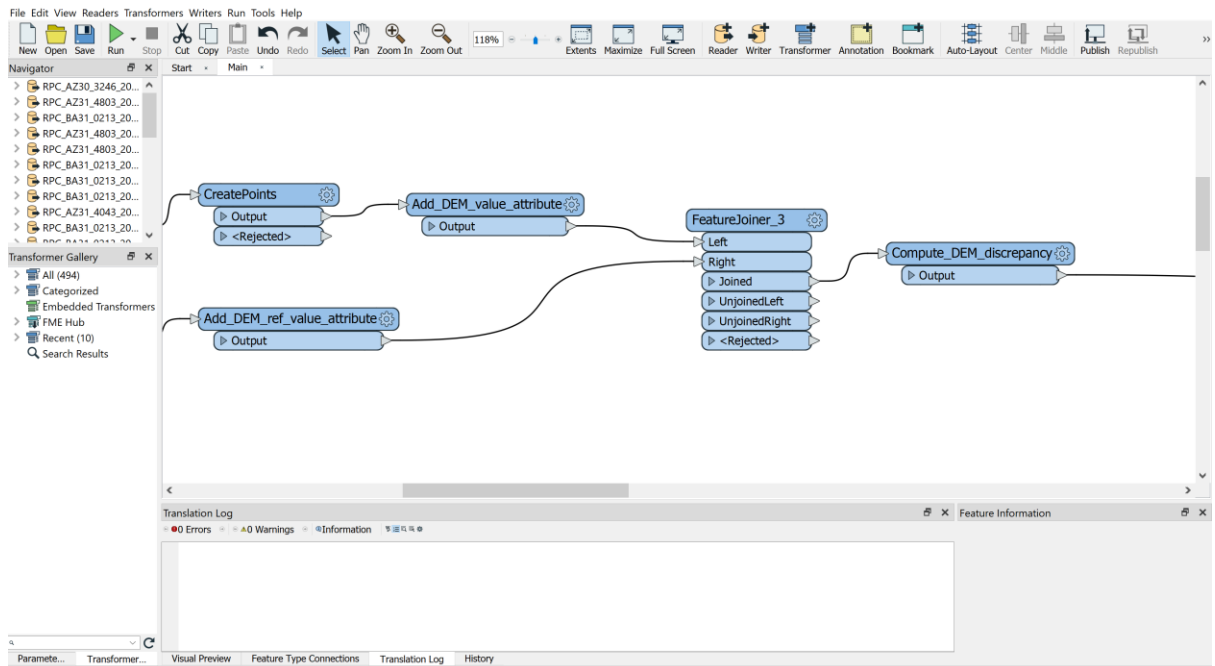


Figure 28: FME

## ArcGIS Pro

ArcGIS Pro is a desktop GIS software from ESRI. It allows data manipulation, publishing, as well as creating visual products (maps, plans). In this project, ArcGIS Pro has been used to inspect and visualize data and create some of the figures for this report. More about this software package can be viewed on Esri’s website: <https://www.esri.com/en-us/arcgis/products/arcgis-pro/overview>.

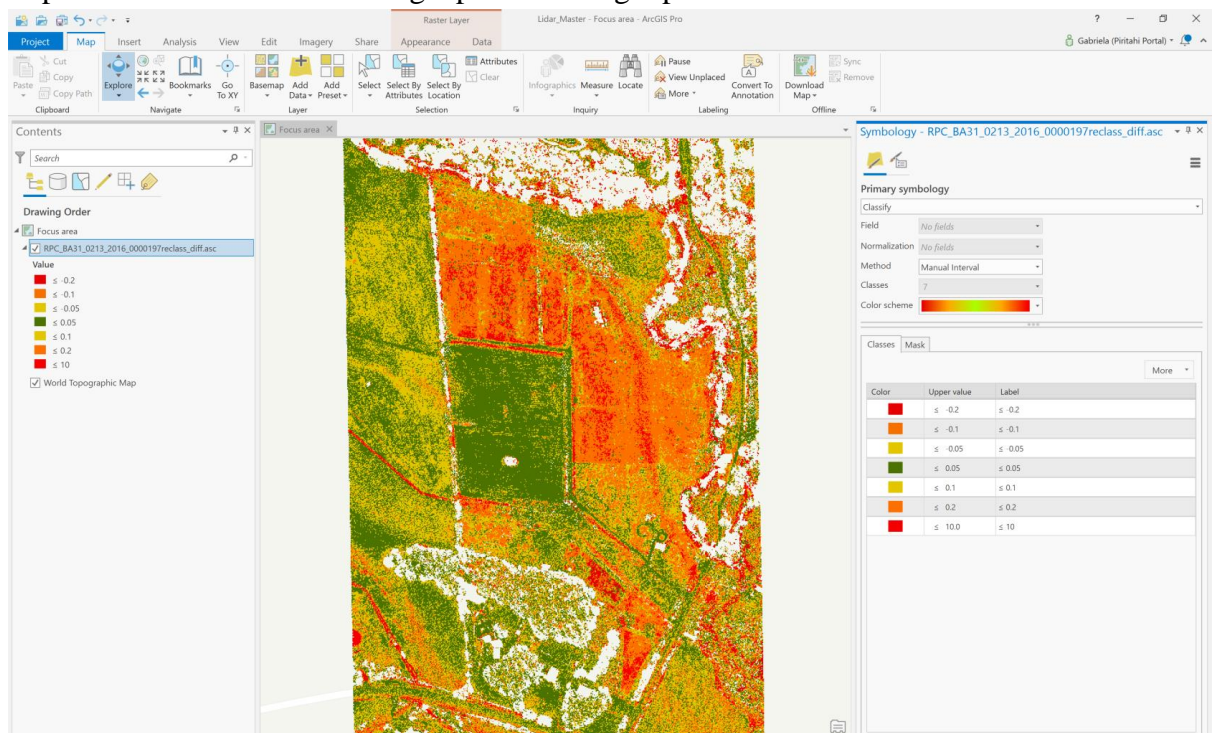


Figure 29: ArcGIS Pro

## Microsoft Excel

Excel spreadsheets have been used to interrogate numerical data outputs and analyse correlations.

## Licensing

Some of the above software packages are freely available – these include Displaz, FugroViewer and Notepad ++. Others have been accessed using licenses acquired by Wood & Partners Consultants Ltd.

## Other notes

The above-mentioned software packages have been used in this project due to their availability/familiarity. Other software packages might have been used to produce similar or the same results. Moreover, few of these programs have overlapping functionality, and on some occasions, the decision on which software to use in which circumstances was based solely on a personal preference.

## Appendix D

Detailed methodology.

### Workflow – ArcGIS Pro

The first step of the workflow was creating a polygon shapefile (named “TestAreas”) and adding features that intersected with low vegetation areas as described in section “Data selection”. Spatial join geoprocessing tool (with 1 to many setting) was then used to output information of all Lidar tiles that intersected the “TestAreas”. Maximum of 4 tiles intersected any selected polygon. New field (“directory”) was added to the resulting feature class, and file directory of each tile was computed using field calculator ('E:/2016AKL\_LiDAR/MtEdenAUK46/RPC\_'+!Name!+'.laz'). Resulting list of file directories has been copied to a text file “listoftiles.txt”. Both the shapefile and the text file are used in processes outlined in the next section.

| id | Name           | Company            | CaptureDate            | Accuracy            | Project                | OBJECTID | DEM | DSM | RPC | BareEarth | AboveGroun | SHAPELeng | SHAPEArea | Directory   |
|----|----------------|--------------------|------------------------|---------------------|------------------------|----------|-----|-----|-----|-----------|------------|-----------|-----------|---|
| 1  | AZ30_3247_2016 | Aerial Surveys Ltd | 30-1-2017, 22-5-2017   | Horizontal +/- 0.3m | Auckland Region 201... | 8911     | 1   | 1   | 1   | 1         | 1          | 2400      | 345600    | E:/2016AKL_LiDAR/MtEdenAUK46/RPC_AZ30_3247_2016.laz |
| 1  | AZ30_3246_2016 | Aerial Surveys Ltd | 30-1-2017, 22-5-2017   | Horizontal +/- 0.3m | Auckland Region 201... | 7534     | 1   | 1   | 1   | 1         | 1          | 2400      | 345600    | E:/2016AKL_LiDAR/MtEdenAUK46/RPC_AZ30_3246_2016.laz |
| 2  | BA31_0213_2016 | Aerial Surveys Ltd | 30-12-2016, 30-7-20... | Horizontal +/- 0.3m | Auckland Region 201... | 13966    | 1   | 1   | 1   | 1         | 1          | 2400      | 345600    | E:/2016AKL_LiDAR/MtEdenAUK46/RPC_BA31_0213_2016.laz |
| 2  | BA31_0212_2016 | Aerial Surveys Ltd | 30-12-2016, 30-7-20... | Horizontal +/- 0.3m | Auckland Region 201... | 14136    | 1   | 1   | 1   | 1         | 1          | 2400      | 345600    | E:/2016AKL_LiDAR/MtEdenAUK46/RPC_BA31_0212_2016.laz |
| 3  | AZ31_4803_2016 | Aerial Surveys Ltd | 23-11-2016, 30-12-2... | Horizontal +/- 0.3m | Auckland Region 201... | 7944     | 1   | 1   | 1   | 1         | 1          | 2400      | 345600    | E:/2016AKL_LiDAR/MtEdenAUK46/RPC_AZ31_4803_2016.laz |
| 4  | AZ31_4043_2016 | Aerial Surveys Ltd | 05-1-2017, 09-6-2017   | Horizontal +/- 0.3m | Auckland Region 201... | 3519     | 1   | 1   | 1   | 1         | 1          | 2400      | 345600    | E:/2016AKL_LiDAR/MtEdenAUK46/RPC_AZ31_4043_2016.laz |
| 4  | AZ31_4043_2016 | Aerial Surveys Ltd | 05-1-2017, 04-2-2017   | Horizontal +/- 0.3m | Auckland Region 201... | 7158     | 1   | 1   | 1   | 1         | 1          | 2400      | 345600    | E:/2016AKL_LiDAR/MtEdenAUK46/RPC_AZ31_4043_2016.laz |
| 4  | AZ31_4143_2016 | Aerial Surveys Ltd | 05-1-2017, 09-6-2017   | Horizontal +/- 0.3m | Auckland Region 201... | 11071    | 1   | 1   | 1   | 1         | 1          | 2400      | 345600    | E:/2016AKL_LiDAR/MtEdenAUK46/RPC_AZ31_4143_2016.laz |
| 4  | AZ31_4143_2016 | Aerial Surveys Ltd | 22-11-2016, 05-1-20... | Horizontal +/- 0.3m | Auckland Region 201... | 15462    | 1   | 1   | 1   | 1         | 1          | 2400      | 345600    | E:/2016AKL_LiDAR/MtEdenAUK46/RPC_AZ31_4143_2016.laz |
| 5  | AZ30_4745_2016 | Aerial Surveys Ltd | 23-11-2016, 06-2-20... | Horizontal +/- 0.3m | Auckland Region 201... | 6948     | 1   | 1   | 1   | 1         | 1          | 2400      | 345600    | E:/2016AKL_LiDAR/MtEdenAUK46/RPC_AZ30_4745_2016.laz |
| 6  | BA31_0431_2016 | Aerial Surveys Ltd | 30-7-2017, 09-10-20... | Horizontal +/- 0.3m | Auckland Region 201... | 4129     | 1   | 1   | 1   | 1         | 1          | 2400      | 345600    | E:/2016AKL_LiDAR/MtEdenAUK46/RPC_BA31_0431_2016.laz |
| 7  | BA32_3209_2016 | Aerial Surveys Ltd | 17-12-2016, 20-12-2... | Horizontal +/- 0.3m | Auckland Region 201... | 5239     | 1   | 1   | 1   | 1         | 1          | 2400      | 345600    | E:/2016AKL_LiDAR/MtEdenAUK46/RPC_BA32_3209_2016.laz |
| 7  | BA32_3109_2016 | Aerial Surveys Ltd | 17-12-2016, 20-12-2... | Horizontal +/- 0.3m | Auckland Region 201... | 16744    | 1   | 1   | 1   | 1         | 1          | 2400      | 345600    | E:/2016AKL_LiDAR/MtEdenAUK46/RPC_BA32_3109_2016.laz |
| 8  | BA31_4749_2016 | Aerial Surveys Ltd | 10-9-2016, 28-1-201... | Horizontal +/- 0.3m | Auckland Region 201... | 3781     | 1   | 1   | 1   | 1         | 1          | 2400      | 345600    | E:/2016AKL_LiDAR/MtEdenAUK46/RPC_BA31_4749_2016.laz |
| 8  | BA31_4748_2016 | Aerial Surveys Ltd | 10-9-2016, 28-1-201... | Horizontal +/- 0.3m | Auckland Region 201... | 11380    | 1   | 1   | 1   | 1         | 1          | 2400      | 345600    | E:/2016AKL_LiDAR/MtEdenAUK46/RPC_BA31_4748_2016.laz |
| 8  | BA31_4649_2016 | Aerial Surveys Ltd | 28-1-2017, 25-4-201... | Horizontal +/- 0.3m | Auckland Region 201... | 11901    | 1   | 1   | 1   | 1         | 1          | 2400      | 345600    | E:/2016AKL_LiDAR/MtEdenAUK46/RPC_BA31_4649_2016.laz |
| 8  | BA31_4648_2016 | Aerial Surveys Ltd | 28-1-2017, 25-4-201... | Horizontal +/- 0.3m | Auckland Region 201... | 18465    | 1   | 1   | 1   | 1         | 1          | 2400      | 345600    | E:/2016AKL_LiDAR/MtEdenAUK46/RPC_BA31_4648_2016.laz |
| 9  | BA32_3602_2016 | Aerial Surveys Ltd | 20-12-2016, 26-4-20... | Horizontal +/- 0.3m | Auckland Region 201... | 2791     | 1   | 1   | 1   | 1         | 1          | 2400      | 345600    | E:/2016AKL_LiDAR/MtEdenAUK46/RPC_BA32_3602_2016.laz |
| 9  | BA32_3601_2016 | Aerial Surveys Ltd | 20-12-2016, 26-4-20... | Horizontal +/- 0.3m | Auckland Region 201... | 15840    | 1   | 1   | 1   | 1         | 1          | 2400      | 345600    | E:/2016AKL_LiDAR/MtEdenAUK46/RPC_BA32_3601_2016.laz |
| 10 | BB32_0316_2016 | AAH NZ Ltd         | 23-10-2016             | Horizontal +/- 0.3m | Auckland Region 201... | 15377    | 1   | 1   | 1   | 1         | 1          | 2400      | 345600    | E:/2016AKL_LiDAR/MtEdenAUK46/RPC_BB32_0316_2016.laz |

Figure 30: Tiles intersecting test areas - ArcGIS Pro table view

### Workflow – LAStools – Methodology 1

#### Copy laz files

Firstly, appropriate laz files were copied to a new directory. List of tiles in text form has been placed in the same folder as batch files and PowerShell has been opened from the same directory.

The inputs in this step include text file created in previous step (using ArcGIS Pro) and original laz files.

Below figure shows the contents of batch file 1\_CopyLaz.bat. Input directory is a folder with all available Lidar laz files. Output directory is selected (it gets created when file is executed). Source and target coordinate systems and vertical datum are set (no reprojection takes place so it is really a house-keeping part of the script, however, it also ensures that when numerical values are used in subsequent scripts, the metric system is used). In lines 10 to 12 the output directory (if pre-existing) including subdirectories gets deleted in silent mode (without requiring confirmation) and then empty new output directory gets created. It is part of most of used scripts, and was useful when trying different settings, re-running batch files etc. Finally, LAStools are called: las2las command is used, with settings to use contents of text file for list of files, specified source and target coordinate systems, specified output directory and an output in laz format.

```

3 set inputdir="E:\2016AKL_LiDAR\MtEdenAUK46"
4 set outdir="E:\Lidar_Master\Processing_LasTools\TestAreas\LazUnclipped"
5
6 set scsys=2105
7 set tcsys=2105
8 set datumtag=AVD46
9
10 rmdir %outdir% /s /q
11 TIMEOUT 1
12 mkdir %outdir%
13
14 las2las -lof listoftiles.txt ^
15         -epsg %scsys% ^
16         -target_epsg %tcsys% ^
17         -odir %outdir% ^
18         -olaz

```

Figure 31: 1\_CopyLaz.bat

Using batch file for copying files is quicker than manually copying each one, is scalable (larger areas, bigger number of files could easily be copied if required) and reduces possibility of human error.

### Clip laz files

In the second step, shapefile with area extents (created as described in previous section - “Data selection”) is used to clip laz files: file with clipping extent is firstly defined in line 3 and then used as input in line 13. Lasclip function is using all laz files in input directory as input, and outputs clipped data in laz format.

```

3 set clipextent="E:\Lidar_Master\Processing_LasTools\TestAreas\TestAreas.shp"
4
5 set indir="E:\Lidar_Master\Processing_LasTools\TestAreas\LazUnclipped"
6 set outdir="E:\Lidar_Master\Processing_LasTools\TestAreas\LazClipped"
7
8 rmdir %outdir% /s /q
9 mkdir %outdir%
10
11
12 lasclip -i %indir%\*.laz ^
13         -poly %clipextent% ^
14         -odir %outdir% ^
15         -olaz
16

```

Figure 32: 2\_ClipLazByShp.bat

Output files from this step are used both in steps: “Create DEMs (original classification)” and “Split flightlines”.

### Create DEMs (original classification)

Las2dem function was used to create digital elevation model files based on clipped laz data. Again, all laz files from stated input directory were used as input. Setting multiple cores was used to speed up the processing. Only class 2 (ground) was used to create the DEM. Step defines the resolution of 5m. Elevation was used to write values to a raster (other options include slope, intensity and more). Output format was set to ascii. No supporting KML file was produced. Output files were assigned a suffix “\_DEM5m\_orig” for easy recognition.



```

2 set datumtag=AVD46
3 set indir="E:\Lidar_Master\Processing_LasTools\TestAreas\LazClipped"
4 set outdir="E:\Lidar_Master\Processing_LasTools\TestAreas\DEMs\OrigFiles"
5
6 rmdir %outdir% /s /q
7 TIMEOUT 1
8 mkdir %outdir%
9
10 set Cores=10
11
12
13 las2dem -i %indir%\*.laz ^
14         -cores %Cores% ^
15         -odir %outdir% ^
16         -epsg 2105 ^
17         -keep_class 2 ^
18         -step 5.0 ^
19         -elevation ^
20         -oasc ^
21         -no_kml ^
22         -odix _DEM5m_orig ^
23

```

Figure 33: 3\_CreateDEMs\_orig.bat

Las2dem function uses point cloud to temporarily triangulate a (high resolution) surface and then rasterises that tin to a user specified resolution raster – therefore individual points/cells (centre values) are not less accurate when step is increased – just smaller in numbers.

## Split flightlines

Clipped laz files were also used as input in “lassplit” function, that separated each laz file into multiple files, based on their point source ID, which is related to individual flight lines (default in this function).

```
3 set datumtag=AVD46
4 set indir="E:\Lidar_Master\Processing_LasTools\TestAreas\LazClipped"
5 set outdir="E:\Lidar_Master\Processing_LasTools\TestAreas\LAZ_flightlines"
6
7 rmdir %outdir% /s /q
8 TIMEOUT 1
9 mkdir %outdir%
10
11 set Cores=10
12
13
14 lassplit -i %indir%\*.laz ^
15          -olaz ^
16          -cores %Cores% ^
17          -odir %outdir% ^
18          -epsg 2105 ^
19
```

Figure 34: 4\_SplitFlightLines.bat

The idea is to derive information from individual flight lines and compare this data to discrepancy between DEM created from individual flight and original DEM (produced as described in “Create DEMs (original classification)” section).

## Reclassify ground

Lasground is a tool for bare earth extraction – it classifies points into ground and non-ground (in line 16, option to leave non-ground points in their original classification is used). By default, only last return is taken into consideration. Most important setting included below – an offset – has been selected to be 0.05 - it sets a tolerance of distance above ground estimate (ground points form a layer rather than flat surface of no thickness, due to survey accuracy, and offset relates to the allowable thickness of that layer). If the number is set too low, it will cause small number of points to meet the criteria, while if it is set too high, low vegetation is likely to be misclassified as bare earth. 0.05 is a reasonable offset to use considering aerial Lidar accuracy.

```
3 set datumtag=AVD46
4 set indir="E:\Lidar_Master\Processing_LasTools\TestAreas\LAZ_flightlines"
5 set outdir="E:\Lidar_Master\Processing_LasTools\TestAreas\LAZ_flightlines_reclass"
6
7 rmdir %outdir% /s /q
8 TIMEOUT 1
9 mkdir %outdir%
10
11 set Cores=10
12
13
14 lasground_new64 -i %indir%\*.laz ^
15                -olaz ^
16                -non_ground_unchanged ^
17                -cores %Cores% ^
18                -odir %outdir% ^
19                -offset 0.05 ^
20                -epsg 2105 ^
21                -odix reclass ^

```

Figure 35: 5\_Reclassify.bat

While different software and more sophisticated methods were used to originally classify point cloud for Auckland Council, before it was passed on to users, the

geometry of points was still at core of that classification, and therefore it is believed that this reclassification (although more simplistic) and extraction of further products will result in valuable material for analysis.

### Create DEMs (reclassified individual flight lines)

Laz files with reclassified, individual flight lines, were used to create a series of DEMs, similarly as described in section “Create DEMs (original classification)”.

```

3 set datumtag=AVD46
4 set indir="E:\Lidar_Master\Processing_LasTools\TestAreas\LAZ_flightlines_reclass"
5 set outdir="E:\Lidar_Master\Processing_LasTools\TestAreas\DEMs\Flightlines"
6
7 rmdir %outdir% /s /q
8 TIMEOUT 1
9 mkdir %outdir%
10
11 set Cores=10
12
13
14 las2dem -i %indir%\*.laz ^
15         -cores %Cores% ^
16         -odir %outdir% ^
17         -epsg 2105 ^
18         -keep_class 2 ^
19         -step 5.0 ^
20         -elevation ^
21         -oasc ^
22         -no_kml ^
23         -odix _DEM5m_flightlinesreclass ^

```

Figure 36: 6\_CreateDEMs\_FlightlinesReclass.bat

The absolute difference between cell values of rasters created in this step and values created based on original data, will be used as a measure of accuracy in the analysis.

### Adaptive thin and point count

One of examined properties was roughness of point cloud representing ground. To test it, adaptive thinning of point cloud was used. Adaptive thinning is a function that can typically be used to decrease the size of data without compromising accuracy too much, by removing points that are not contributing to a change of tin by more than a selected by user tolerance. It is a very useful tool when needing to use the data in software not designed to handle (typically very large) point clouds. Consider figure 37: if selected vertical tolerance is set to a very low value, both green and blue points would remain; if tolerance is set a bit higher, green point would be removed from point cloud while blue one would remain; and if tolerance is very high, both green and blue points would be removed (and data size most reduced). The higher the tolerance, the lower the subsequent products accuracy, and the lower the number of points in output point cloud. On flat areas (or, rather, on those of consistent slope), even thinning with low tolerance can reduce amount (and size) of data drastically.



Figure 37: Adaptive thinning supporting graphic

In this experiment, thinning algorithm is tested with 3 different tolerances: 0.1, 0.05 and 0.025m, and later the number of remaining points in regular grid cells is counted. The rougher the surface, the more points should remain after thinning. The reason for

this test was to see if low vegetation wrongly classified as ground would show different (stronger) height variation (rougher point cloud).

One thing to note here is that thinning is influenced by reclassification offset tolerance described in “Reclassify” section – point cloud will appear less rough if low offset was used.

```
2 set datumtag=AVD46
3 set indir="E:\Lidar_Master\Processing_LasTools\TestAreas\LAZ_flightlines_reclass"
4 set outdir="E:\Lidar_Master\Processing_LasTools\TestAreas\AdaptiveThin\01_05"
5
6 rmdir %outdir% /s /q
7 TIMEOUT 1
8 mkdir %outdir%
9
10 set Cores=10
11
12
13 lasthin -i %indir%\*.laz ^
14         -cores %Cores% ^
15         -odir %outdir% ^
16         -epsg 2105 ^
17         -adaptive 0.1 5 ^
18         -keep_class 2 ^
19         -olaz ^
20         -odix _Thin_01_5 ^
```

Figure 38: 7\_AdaptiveThin\_01\_05.bat

Script shown on the figure above was used to execute the lasthin function. Both input and output are in laz format. The most important setting, as explained above, is the “adaptive”: 0.1 has been selected for the vertical tolerance, and 5 is the maximum allowable spacing between points (this ensures that even on very flat areas, some points are preserved). Identical script was also executed for tolerances of 0.05 and 0.025 (with changed output directory, output file suffix and obviously a changed adaptive setting). Original (flight separated, reclassified) and thinned out laz files were then used as inputs to point count scripts executed using lasgrid.

```
3 set datumtag=AVD46
4 set indir="E:\Lidar_Master\Processing_LasTools\TestAreas\LAZ_flightlines_reclass"
5 set outdir=
  "E:\Lidar_Master\Processing_LasTools\TestAreas\FlightLinesRasters\Density_Nonfiltered_5m"
6
7 rmdir %outdir% /s /q
8 TIMEOUT 1
9 mkdir %outdir%
10
11 set Cores=10
12
13
14 lasgrid -i %indir%\*.laz ^
15         -cores %Cores% ^
16         -odir %outdir% ^
17         -epsg 2105 ^
18         -step 5.0 ^
19         -keep_class 2 ^
20         -counter_32bit ^
21         -oasc ^
22         -no_kml ^
23         -odix _5mPCCount ^
```

Figure 39: 8\_LasGrid\_PCount\_Orig\_5.bat

```

3 set datumtag=AVD46
4 set indir="E:\Lidar_Master\Processing_LasTools\TestAreas\AdaptiveThin\01_05"
5 set outdir=
  "E:\Lidar_Master\Processing_LasTools\TestAreas\FlightLinesRasters\Density_Thin01_5m"
6
7 rmdir %outdir% /s /q
8 TIMEOUT 1
9 mkdir %outdir%
10
11 set Cores=10
12
13
14 lasgrid -i %indir%\*.laz ^
15         -cores %Cores% ^
16         -odir %outdir% ^
17         -epsg 2105 ^
18         -step 5.0 ^
19         -keep_class 2 ^
20         -counter_32bit ^
21         -oasc ^
22         -no_kml ^
23         -odix Thin01_5mPCount ^

```

Figure 40: 8\_LasGrid\_PCount\_Thin01\_5.bat

2 out of 4 scripts are shown above. Grid distance of 5 was used again, to comply with DEMs and Ascii format was selected for outputs. Point counting scripts that were used, only differ in input and output directories and suffixes.

The products consist of ascii files (plus supporting projection files), where regularly spaced values stand for number of ground points counted within each cell.

## Slope

Slope has been computed using las2dem function, with option to output slope instead of default height. Reclassified individual flight lines point clouds were used as inputs. Outputs, with 5m resolution, have been produced in asc format.

```

3 set datumtag=AVD46
4 set indir="E:\Lidar_Master\Processing_LasTools\TestAreas\LAZ_flightlines_reclass"
5 set outdir="E:\Lidar_Master\Processing_LasTools\TestAreas\FlightLinesRasters\Slopes"
6
7 rmdir %outdir% /s /q
8 TIMEOUT 1
9 mkdir %outdir%
10
11 set Cores=10
12
13
14 las2dem -i %indir%\*.laz ^
15         -cores %Cores% ^
16         -odir %outdir% ^
17         -epsg 2105 ^
18         -step 5.0 ^
19         -keep_class 2 ^
20         -slope ^
21         -oasc ^
22         -no_kml ^
23         -odix Slope5m ^

```

Figure 41: 8\_Las2DEM\_Slope.bat

As mentioned in literature overview (“ALS Accuracy”), it is known that there is a relationship between Lidar accuracy and slope (or more precisely, the angle at which laser beam hits the surface, which is related to slope), however, it may not be visible in this data (see results section).

## Scan angle

Like slope, scan angle is related to (influences) the incidence angle. It has been computed as an average for each cell.

```
3 set datumtag=AVD46
4 set indir="E:\Lidar_Master\Processing_LasTools\TestAreas\LAZ_flightlines_reclass"
5 set outdir="E:\Lidar_Master\Processing_LasTools\TestAreas\FlightLinesRasters\ScanAngleAvg"
6
7 rmdir %outdir% /s /q
8 TIMEOUT 1
9 mkdir %outdir%
10
11 set Cores=10
12
13
14 lasgrid -i %indir%\*.laz ^
15         -cores %Cores% ^
16         -odir %outdir% ^
17         -epsg 2105 ^
18         -step 5.0 ^
19         -scan_angle_abs_average ^
20         -keep_class 2 ^
21         -oasc ^
22         -no_kml ^
23         -odix _ScanAngleAvg ^
```

Figure 42: 8\_LasGrid\_ScanAngleAvg.bat

## Class variety and number of returns

To check if presence of different features, such as man-made structures or higher vegetation influences accuracy, number of different classes present within each cell has also been computed and written to asc files. Because the selected areas were specifically selected to cover low vegetation (with very little class variety), this is just a supplementary test.

```
3 set datumtag=AVD46
4 set indir="E:\Lidar_Master\Processing_LasTools\TestAreas\LAZ_flightlines_reclass"
5 set outdir="E:\Lidar_Master\Processing_LasTools\TestAreas\FlightLinesRasters\ClassificationVariety"
6
7 rmdir %outdir% /s /q
8 TIMEOUT 1
9 mkdir %outdir%
10
11 set Cores=10
12
13
14 lasgrid -i %indir%\*.laz ^
15         -cores %Cores% ^
16         -odir %outdir% ^
17         -epsg 2105 ^
18         -step 5.0 ^
19         -classification_variety ^
20         -oasc ^
21         -no_kml ^
22         -odix _ClassVariety ^
```

Figure 43: 8\_LasGrid\_ClassVar.bat

Average number of returns has also been computed (for points of class 2), and it is related to class variety: if only ground was recorded, the number of returns should be 1 or close to 1, and if other features were recorded, before beam reached the ground, the number would be higher. Interestingly, if class variety suggests presence of different land covers (vegetation on top of ground), but average number of returns is very close

to one, it could mean that each laser beam either recorded vegetation or ground, but not both (did not penetrate through vegetation).

```
3 set datumtag=AVD46
4 set indir="E:\Lidar_Master\Processing_LasTools\TestAreas\LAZ_flightlines_reclass"
5 set outdir=
  "E:\Lidar_Master\Processing_LasTools\TestAreas\FlightLinesRasters>ReturnsNumberAvg"
6
7 rmdir %outdir% /s /q
8 TIMEOUT 1
9 mkdir %outdir%
10
11 set Cores=10
12
13
14 lasgrid -i %indir%\*.laz ^
15         -cores %Cores% ^
16         -odir %outdir% ^
17         -epsg 2105 ^
18         -step 5.0 ^
19         -number_returns_average ^
20         -keep_class 2 ^
21         -oasc ^
22         -no_kml ^
23         -odix _RetNumAvg ^
```

Figure 44: 8\_LasGrid\_RetNumAvg.bat

### Height data

Another point cloud characteristic that was examined, was height related information. Height range was computed for each cell. This is in a way related to slope: the higher the range - the higher the terrain slope; however, larger height range on flat areas could indicate some data issues. Figure 45 pictures the script. Additionally, to height range, height standard deviation within 5x5m cell was computed (Figure 46).

```
3 set datumtag=AVD46
4 set indir="E:\Lidar_Master\Processing_LasTools\TestAreas\LAZ_flightlines_reclass"
5 set outdir="E:\Lidar_Master\Processing_LasTools\TestAreas\FlightLinesRasters\HRange"
6
7 rmdir %outdir% /s /q
8 TIMEOUT 1
9 mkdir %outdir%
10
11 set Cores=10
12
13
14 lasgrid -i %indir%\*.laz ^
15         -cores %Cores% ^
16         -odir %outdir% ^
17         -epsg 2105 ^
18         -step 5.0 ^
19         -elevation_range ^
20         -keep_class 2 ^
21         -oasc ^
22         -no_kml ^
23         -odix _HRange ^
```

Figure 45: 8\_LasGrid\_HRange.bat

```

3 set datumtag=AVD46
4 set indir="E:\Lidar_Master\Processing_LasTools\TestAreas\LAZ_flightlines_reclass"
5 set outdir="E:\Lidar_Master\Processing_LasTools\TestAreas\FlightLinesRasters\HStdDev"
6
7 rmdir %outdir% /s /q
8 TIMEOUT 1
9 mkdir %outdir%
10
11 set Cores=10
12
13
14 lasgrid -i %indir%\*.laz ^
15         -cores %Cores% ^
16         -odir %outdir% ^
17         -epsg 2105 ^
18         -step 5.0 ^
19         -elevation_stddev ^
20         -keep_class 2 ^
21         -oasc ^
22         -no_kml ^
23         -odix _HStdDev ^

```

Figure 46: 8\_LasGrid\_HStdDev.bat

### Intensity

Intensity of Lidar points was also amongst the focus of analysis. Intensity is recorded for each point and according to “Methods from information extraction from LIDAR intensity data and multispectral LIDAR technology” (2018, Scaioni M., Höfle B., Baungarten Kersting A.P., Barazzetti L., Previtali M., Wujanz D.), it can help with data classification. Intensity depends on variety of factors, but one of the main ones is the number of returns: the same surface under the same conditions will return points of different intensity, if part of the beam has been already reflected by different object(s), and therefore not full portion has reached and bounced off that surface. To remove this major factor, only the points that had been recorded with laser beam that had only 1 return (“keep\_number\_of\_returns 1” option) have been used to compute intensity range (Figure 47), average intensity (Figure 48) and intensity standard deviation (Figure 49).

```

3 set datumtag=AVD46
4 set indir="E:\Lidar_Master\Processing_LasTools\TestAreas\LAZ_flightlines_reclass"
5 set outdir="E:\Lidar_Master\Processing_LasTools\TestAreas\FlightLinesRasters\IntensityRange"
6
7 rmdir %outdir% /s /q
8 TIMEOUT 1
9 mkdir %outdir%
10
11 set Cores=10
12
13
14 lasgrid -i %indir%\*.laz ^
15         -cores %Cores% ^
16         -odir %outdir% ^
17         -epsg 2105 ^
18         -step 5.0 ^
19         -intensity_range ^
20         -keep_class 2 ^
21         -keep_number_of_returns 1 ^
22         -oasc ^
23         -no_kml ^
24         -odix _IntensityRange ^

```

Figure 47: 8\_LasGrid\_IntensityRange.bat



```

3 set datumtag=AVD46
4 set indir="E:\Lidar_Master\Processing_LasTools\TestAreas\LAZ_flightlines_reclass"
5 set outdir="E:\Lidar_Master\Processing_LasTools\TestAreas\FlightLinesRasters\IntensityAvg"
6
7 rmdir %outdir% /s /q
8 TIMEOUT 1
9 mkdir %outdir%
10
11 set Cores=10
12
13
14 lasgrid -i %indir%\*.laz ^
15         -cores %Cores% ^
16         -odir %outdir% ^
17         -epsg 2105 ^
18         -step 5.0 ^
19         -intensity_average ^
20         -keep_class 2 ^
21         -keep_number_of_returns 1 ^
22         -oasc ^
23         -no_kml ^
24         -odix IntensityAvg ^

```

Figure 48: 8\_LasGrid\_IntensityAvg.bat

```

3 set datumtag=AVD46
4 set indir="E:\Lidar_Master\Processing_LasTools\TestAreas\LAZ_flightlines_reclass"
5 set outdir="E:\Lidar_Master\Processing_LasTools\TestAreas\FlightLinesRasters\IntensityStdDev"
6
7 rmdir %outdir% /s /q
8 TIMEOUT 1
9 mkdir %outdir%
10
11 set Cores=10
12
13
14 lasgrid -i %indir%\*.laz ^
15         -cores %Cores% ^
16         -odir %outdir% ^
17         -epsg 2105 ^
18         -step 5.0 ^
19         -intensity_stddev ^
20         -keep_class 2 ^
21         -keep_number_of_returns 1 ^
22         -oasc ^
23         -no_kml ^
24         -odix _IntensityStdDev ^

```

Figure 49: 8\_LasGrid\_IntensityStdDev.bat

## Workflow – LAStools – Methodology 2

Second analysis approach used a subset of data created by 4\_SplitFlightLines.bat script, that was followed by:

- Adaptive thin and point cloud for class 2 and class 3 separately
- Height range, height standard deviation, intensity (average, range and standard deviation) for class 2 and class 3 separately

Scripts used in the second analysis approach are identical to those in the methodology 1 and differ mostly in input/output directories. “Keep\_class” function is used to create outputs for classes 2 and 3.

## Workflow – FME

Chart below (Figure 50) provides a summary of methodology 1 data processing using FME. Firstly, each ascii file gets converted to points, x and y values are written to attributes and so is the raster value (appropriate attribute names are assigned, such as “Height\_Range”, Intensity\_Average” etc.). Original DEM values are (inner) joined to each reclassified DEM value (based on X and Y attributes) and then the absolute difference in Z values between the DEMs is computed for each point. In the meantime, all point cloud characteristics raster datasets were joined with each other in a series of succeeding outer joins (outer joins are used to still retain points that would fail to have

some of the values, for example when data was filtered on “keep\_number\_of\_returns 1” asc file would include null values when all ground points in a cell were a result of second or higher return). Points with combined point cloud characteristics, now written into specific attributes, were then joined to DEM points (again, based on x, y). Finally, all points were written into an ESRI file geodatabase as point feature classes: one class per each file with separated flight passes for easy identification of data origin.

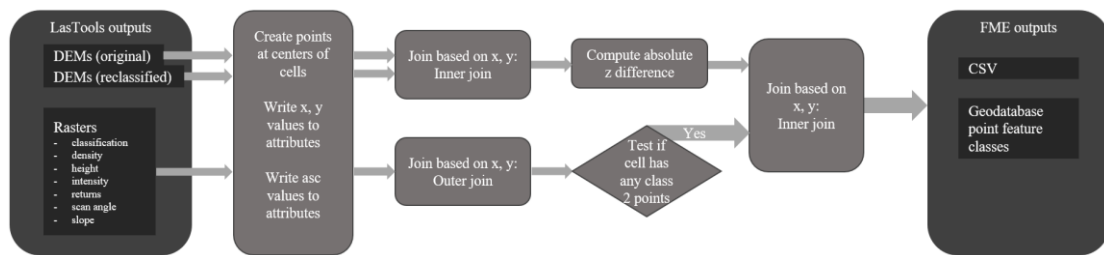


Figure 50: FME workflow Methodology 1

Figure below pictures an FME workbench designed to carry out the process as described above. On the left, there are “readers” – source files (one reader has been set for each ascii file type, for example class variety rasters are in one reader, and original density rasters are in another reader). FME transformers are symbolised by blue colour – these are various processing tools (for example attribute creators, value extractors, feature joiners, testers). On the right, there are “writers” – tools that export prepared data to specified formats (in this case, point feature classes in gdb and a csv file).

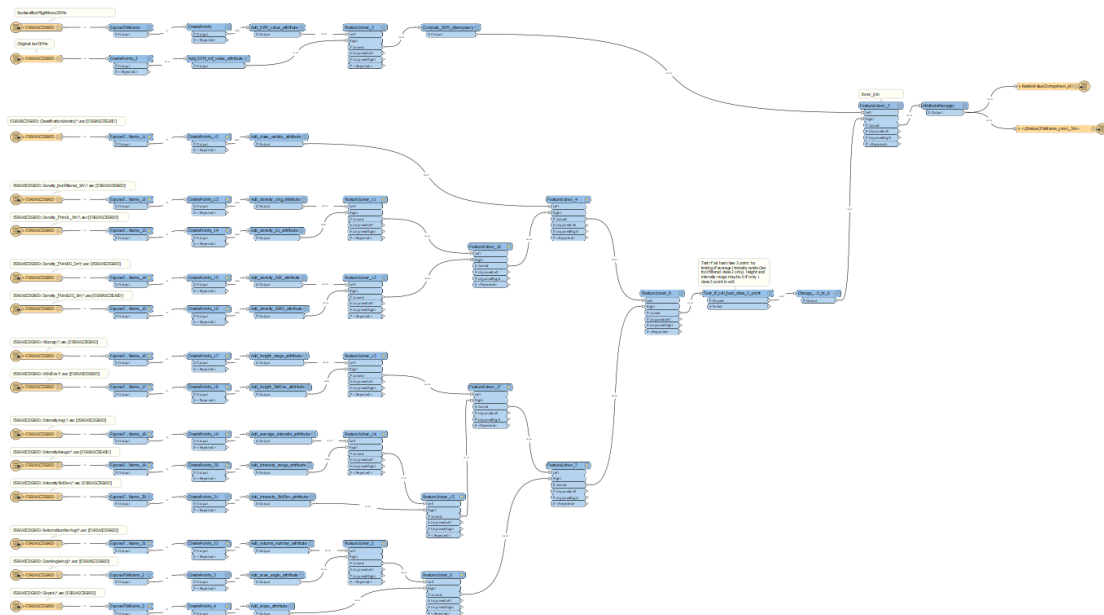


Figure 51: FME workbench (Methodology 1)

Methodology 2 data processing is shown in the flowchart below. Uniformly to the first approach, points are getting derived from asc files and joined based on their location. This time, no join to DEM is needed. Outputs have been filtered to ignore cells with below 5 points (original point count) as computing standard deviations or ranges on very small number of points is not desirable. The process shown below has been followed twice (once for each of the two analysed classes).

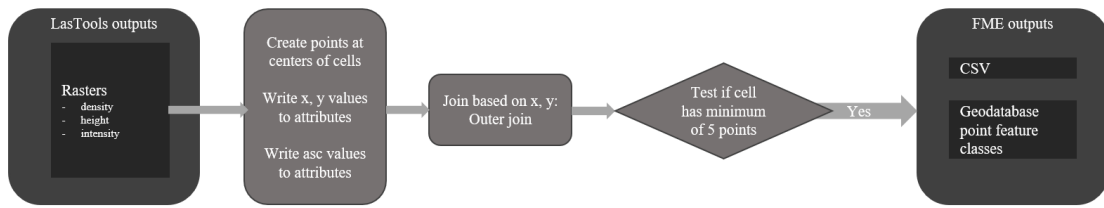


Figure 52: FME workflow Methodology 2

FME workbench used in Methodology 2 can be seen below.

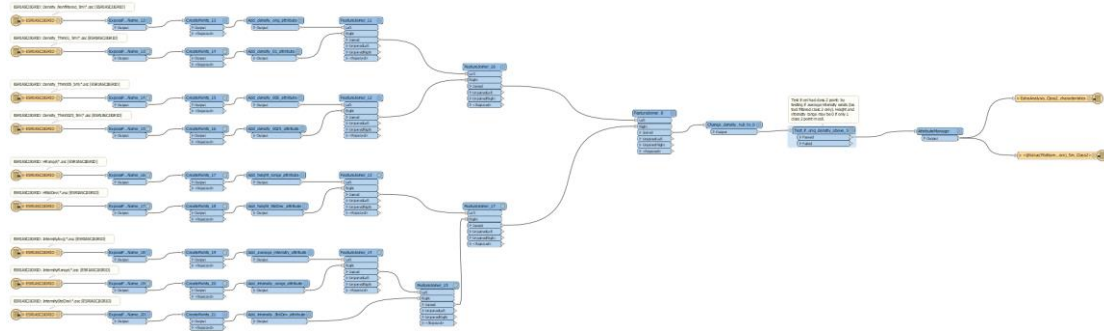


Figure 53: FME workbench (Methodology 2)

# Appendix E

Auckland Council
Map

**Place Names**

**Place Name (500,000)**  
Place Name (500,000)

**Place Name Search**  
Place Name Search

**Rail Stations**

**Railway Lines**

**Auckland Council Boundary**  
— Auckland Council Boundary

**Roads**

**Property**  
Property

**Rate Assessment**  
Rate Assessment

**Coastline**

**New Zealand (1,000,000)**  
 New Zealand (1,000,000)

**Base Region Auckland Council (5m)**

Land Outside

Water

**Ward**  
 Ward

**Region Cache Public Open Space Extent**  
 Region Cache Public Open Space Extent

**LIDAR2006 1m DEM Hillshade**

High : 254 - Low : 0

**NZ Hillshade**

High : 254 - Low : 0

**DISCLAIMER**  
This map/plan is illustrative only and all information should be independently verified on site before taking any action.  
Copyright Auckland Council. Land Parcel Boundary information from LINZ (Crown Copyright Reserved). Whilst due care has been taken, Auckland Council gives no warranty as to the accuracy and plan completeness of any information on this map/plan and accepts no liability for any error, omission or use of the information. Height datum: Auckland 1986.

**Legend**

**Date Printed:**  
7/11/2021



public

**DISCLAIMER:**  
This map/plan is illustrative only and all information should be independently verified on site before taking any action. Copyright Auckland Council. Land Parcel Boundary information from LINZ (Crown Copyright Reserved). Whilst due care has been taken, Auckland Council gives no warranty as to the accuracy and plan completeness of any information on this map/plan and accepts no liability for any error, omission or use of the information. Height datum: Auckland 1946.

# Auckland Council's Land

0 4,800 9,600 14,400  
Meters  
**Scale @ A4**  
= 1:1,000,000  
**Date Printed:**  
7/11/2021





Series from Lund University

## **Department of Physical Geography and Ecosystem Science**

### **Master Thesis in Geographical Information Science**

1. *Anthony Lawther*: The application of GIS-based binary logistic regression for slope failure susceptibility mapping in the Western Grampian Mountains, Scotland (2008).
2. *Rickard Hansen*: Daily mobility in Grenoble Metropolitan Region, France. Applied GIS methods in time geographical research (2008).
3. *Emil Bayramov*: Environmental monitoring of bio-restoration activities using GIS and Remote Sensing (2009).
4. *Rafael Villarreal Pacheco*: Applications of Geographic Information Systems as an analytical and visualization tool for mass real estate valuation: a case study of Fontibon District, Bogota, Columbia (2009).
5. *Siri Oestreich Waage*: a case study of route solving for oversized transport: The use of GIS functionalities in transport of transformers, as part of maintaining a reliable power infrastructure (2010).
6. *Edgar Pimiento*: Shallow landslide susceptibility – Modelling and validation (2010).
7. *Martina Schäfer*: Near real-time mapping of floodwater mosquito breeding sites using aerial photographs (2010).
8. *August Pieter van Waarden-Nagel*: Land use evaluation to assess the outcome of the programme of rehabilitation measures for the river Rhine in the Netherlands (2010).
9. *Samira Muhammad*: Development and implementation of air quality data mart for Ontario, Canada: A case study of air quality in Ontario using OLAP tool. (2010).
10. *Fredros Oketch Okumu*: Using remotely sensed data to explore spatial and temporal relationships between photosynthetic productivity of vegetation and malaria transmission intensities in selected parts of Africa (2011).
11. *Svajunas Plunge*: Advanced decision support methods for solving diffuse water pollution problems (2011).
12. *Jonathan Higgins*: Monitoring urban growth in greater Lagos: A case study using GIS to monitor the urban growth of Lagos 1990 - 2008 and produce future growth prospects for the city (2011).
13. *Mårten Karlberg*: Mobile Map Client API: Design and Implementation for Android (2011).
14. *Jeanette McBride*: Mapping Chicago area urban tree canopy using color infrared imagery (2011).
15. *Andrew Farina*: Exploring the relationship between land surface temperature and vegetation abundance for urban heat island mitigation in Seville, Spain (2011).
16. *David Kanyari*: Nairobi City Journey Planner: An online and a Mobile Application (2011).
17. *Laura V. Drews*: Multi-criteria GIS analysis for siting of small wind power plants - A case study from Berlin (2012).
18. *Qaisar Nadeem*: Best living neighborhood in the city - A GIS based multi criteria evaluation of ArRiyadh City (2012).
19. *Ahmed Mohamed El Saeid Mustafa*: Development of a photo voltaic building rooftop integration analysis tool for GIS for Dokki District, Cairo, Egypt (2012).

20. *Daniel Patrick Taylor*: Eastern Oyster Aquaculture: Estuarine Remediation via Site Suitability and Spatially Explicit Carrying Capacity Modeling in Virginia's Chesapeake Bay (2013).
21. *Angeleta Oveta Wilson*: A Participatory GIS approach to *unearthing* Manchester's Cultural Heritage 'gold mine' (2013).
22. *Ola Svensson*: Visibility and Tholos Tombs in the Messenian Landscape: A Comparative Case Study of the Pylian Hinterlands and the Soulima Valley (2013).
23. *Monika Ogden*: Land use impact on water quality in two river systems in South Africa (2013).
24. *Stefan Rova*: A GIS based approach assessing phosphorus load impact on Lake Flaten in Salem, Sweden (2013).
25. *Yann Buhot*: Analysis of the history of landscape changes over a period of 200 years. How can we predict past landscape pattern scenario and the impact on habitat diversity? (2013).
26. *Christina Fotiou*: Evaluating habitat suitability and spectral heterogeneity models to predict weed species presence (2014).
27. *Inese Linuza*: Accuracy Assessment in Glacier Change Analysis (2014).
28. *Agnieszka Griffin*: Domestic energy consumption and social living standards: a GIS analysis within the Greater London Authority area (2014).
29. *Brynja Guðmundsdóttir*: Detection of potential arable land with remote sensing and GIS - A Case Study for Kjósarhreppur (2014).
30. *Oleksandr Nekrasov*: Processing of MODIS Vegetation Indices for analysis of agricultural droughts in the southern Ukraine between the years 2000-2012 (2014).
31. *Sarah Tressel*: Recommendations for a polar Earth science portal in the context of Arctic Spatial Data Infrastructure (2014).
32. *Caroline Gevaert*: Combining Hyperspectral UAV and Multispectral Formosat-2 Imagery for Precision Agriculture Applications (2014).
33. *Salem Jamal-Uddeen*: Using GeoTools to implement the multi-criteria evaluation analysis - weighted linear combination model (2014).
34. *Samanah Seyedi-Shandiz*: Schematic representation of geographical railway network at the Swedish Transport Administration (2014).
35. *Kazi Masel Ullah*: Urban Land-use planning using Geographical Information System and analytical hierarchy process: case study Dhaka City (2014).
36. *Alexia Chang-Wailing Spitteler*: Development of a web application based on MCDA and GIS for the decision support of river and floodplain rehabilitation projects (2014).
37. *Alessandro De Martino*: Geographic accessibility analysis and evaluation of potential changes to the public transportation system in the City of Milan (2014).
38. *Alireza Mollasalehi*: GIS Based Modelling for Fuel Reduction Using Controlled Burn in Australia. Case Study: Logan City, QLD (2015).
39. *Negin A. Sanati*: Chronic Kidney Disease Mortality in Costa Rica; Geographical Distribution, Spatial Analysis and Non-traditional Risk Factors (2015).
40. *Karen McIntyre*: Benthic mapping of the Bluefields Bay fish sanctuary, Jamaica (2015).
41. *Kees van Duijvendijk*: Feasibility of a low-cost weather sensor network for agricultural purposes: A preliminary assessment (2015).



42. *Sebastian Andersson Hylander*: Evaluation of cultural ecosystem services using GIS (2015).
43. *Deborah Bowyer*: Measuring Urban Growth, Urban Form and Accessibility as Indicators of Urban Sprawl in Hamilton, New Zealand (2015).
44. *Stefan Arvidsson*: Relationship between tree species composition and phenology extracted from satellite data in Swedish forests (2015).
45. *Damián Giménez Cruz*: GIS-based optimal localisation of beekeeping in rural Kenya (2016).
46. *Alejandra Narváez Vallejo*: Can the introduction of the topographic indices in LPJ-GUESS improve the spatial representation of environmental variables? (2016).
47. *Anna Lundgren*: Development of a method for mapping the highest coastline in Sweden using breaklines extracted from high resolution digital elevation models (2016).
48. *Oluwatomi Esther Adejoro*: Does location also matter? A spatial analysis of social achievements of young South Australians (2016).
49. *Hristo Dobrev Tomov*: Automated temporal NDVI analysis over the Middle East for the period 1982 - 2010 (2016).
50. *Vincent Muller*: Impact of Security Context on Mobile Clinic Activities A GIS Multi Criteria Evaluation based on an MSF Humanitarian Mission in Cameroon (2016).
51. *Gezahagn Negash Seboka*: Spatial Assessment of NDVI as an Indicator of Desertification in Ethiopia using Remote Sensing and GIS (2016).
52. *Holly Buhler*: Evaluation of Interfacility Medical Transport Journey Times in Southeastern British Columbia. (2016).
53. *Lars Ole Grottenberg*: Assessing the ability to share spatial data between emergency management organisations in the High North (2016).
54. *Sean Grant*: The Right Tree in the Right Place: Using GIS to Maximize the Net Benefits from Urban Forests (2016).
55. *Irshad Jamal*: Multi-Criteria GIS Analysis for School Site Selection in Gorno-Badakhshan Autonomous Oblast, Tajikistan (2016).
56. *Fulgencio Sanmartín*: Wisdom-volcano: A novel tool based on open GIS and time-series visualization to analyse and share volcanic data (2016).
57. *Nezha Acil*: Remote sensing-based monitoring of snow cover dynamics and its influence on vegetation growth in the Middle Atlas Mountains (2016).
58. *Julia Hjalmarsson*: A Weighty Issue: Estimation of Fire Size with Geographically Weighted Logistic Regression (2016).
59. *Mathewos Tamiru Amato*: Using multi-criteria evaluation and GIS for chronic food and nutrition insecurity indicators analysis in Ethiopia (2016).
60. *Karim Alaa El Din Mohamed Soliman El Attar*: Bicycling Suitability in Downtown, Cairo, Egypt (2016).
61. *Gilbert Akol Echelai*: Asset Management: Integrating GIS as a Decision Support Tool in Meter Management in National Water and Sewerage Corporation (2016).
62. *Terje Slinning*: Analytic comparison of multibeam echo soundings (2016).
63. *Gréta Hlín Sveinsdóttir*: GIS-based MCDA for decision support: A framework for wind farm siting in Iceland (2017).
64. *Jonas Sjögren*: Consequences of a flood in Kristianstad, Sweden: A GIS-based analysis of impacts on important societal functions (2017).

65. *Nadine Raska*: 3D geologic subsurface modelling within the Mackenzie Plain, Northwest Territories, Canada (2017).
66. *Panagiotis Symeonidis*: Study of spatial and temporal variation of atmospheric optical parameters and their relation with PM 2.5 concentration over Europe using GIS technologies (2017).
67. *Michaela Bobeck*: A GIS-based Multi-Criteria Decision Analysis of Wind Farm Site Suitability in New South Wales, Australia, from a Sustainable Development Perspective (2017).
68. *Raghdaa Eissa*: Developing a GIS Model for the Assessment of Outdoor Recreational Facilities in New Cities Case Study: Tenth of Ramadan City, Egypt (2017).
69. *Zahra Khais Shahid*: Biofuel plantations and isoprene emissions in Svea and Götaland (2017).
70. *Mirza Amir Liaquat Baig*: Using geographical information systems in epidemiology: Mapping and analyzing occurrence of diarrhea in urban - residential area of Islamabad, Pakistan (2017).
71. *Joakim Jörwall*: Quantitative model of Present and Future well-being in the EU-28: A spatial Multi-Criteria Evaluation of socioeconomic and climatic comfort factors (2017).
72. *Elin Haettner*: Energy Poverty in the Dublin Region: Modelling Geographies of Risk (2017).
73. *Harry Eriksson*: Geochemistry of stream plants and its statistical relations to soil- and bedrock geology, slope directions and till geochemistry. A GIS-analysis of small catchments in northern Sweden (2017).
74. *Daniel Gardevärn*: PPGIS and Public meetings – An evaluation of public participation methods for urban planning (2017).
75. *Kim Friberg*: Sensitivity Analysis and Calibration of Multi Energy Balance Land Surface Model Parameters (2017).
76. *Viktor Svanerud*: Taking the bus to the park? A study of accessibility to green areas in Gothenburg through different modes of transport (2017).
77. *Lisa-Gaye Greene*: Deadly Designs: The Impact of Road Design on Road Crash Patterns along Jamaica's North Coast Highway (2017).
78. *Katarina Jemec Parker*: Spatial and temporal analysis of fecal indicator bacteria concentrations in beach water in San Diego, California (2017).
79. *Angela Kabiru*: An Exploratory Study of Middle Stone Age and Later Stone Age Site Locations in Kenya's Central Rift Valley Using Landscape Analysis: A GIS Approach (2017).
80. *Kristean Björkmann*: Subjective Well-Being and Environment: A GIS-Based Analysis (2018).
81. *Williams Erhunmonmen Ojo*: Measuring spatial accessibility to healthcare for people living with HIV-AIDS in southern Nigeria (2018).
82. *Daniel Assefa*: Developing Data Extraction and Dynamic Data Visualization (Styling) Modules for Web GIS Risk Assessment System (WGRAS). (2018).
83. *Adela Nistora*: Inundation scenarios in a changing climate: assessing potential impacts of sea-level rise on the coast of South-East England (2018).
84. *Marc Seliger*: Thirsty landscapes - Investigating growing irrigation water consumption and potential conservation measures within Utah's largest master-planned community: Daybreak (2018).
85. *Luka Jovičić*: Spatial Data Harmonisation in Regional Context in Accordance with INSPIRE Implementing Rules (2018).

86. *Christina Kourdounouli*: Analysis of Urban Ecosystem Condition Indicators for the Large Urban Zones and City Cores in EU (2018).
87. *Jeremy Azzopardi*: Effect of distance measures and feature representations on distance-based accessibility measures (2018).
88. *Patrick Kabatha*: An open source web GIS tool for analysis and visualization of elephant GPS telemetry data, alongside environmental and anthropogenic variables (2018).
89. *Richard Alphonse Giliba*: Effects of Climate Change on Potential Geographical Distribution of *Prunus africana* (African cherry) in the Eastern Arc Mountain Forests of Tanzania (2018).
90. *Eiður Kristinn Eiðsson*: Transformation and linking of authoritative multi-scale geodata for the Semantic Web: A case study of Swedish national building data sets (2018).
91. *Niamh Harty*: HOP!: a PGIS and citizen science approach to monitoring the condition of upland paths (2018).
92. *José Estuardo Jara Alvear*: Solar photovoltaic potential to complement hydropower in Ecuador: A GIS-based framework of analysis (2018).
93. *Brendan O'Neill*: Multicriteria Site Suitability for Algal Biofuel Production Facilities (2018).
94. *Roman Spataru*: Spatial-temporal GIS analysis in public health – a case study of polio disease (2018).
95. *Alicja Miodońska*: Assessing evolution of ice caps in Suðurland, Iceland, in years 1986 - 2014, using multispectral satellite imagery (2019).
96. *Dennis Lindell Schettini*: A Spatial Analysis of Homicide Crime's Distribution and Association with Deprivation in Stockholm Between 2010-2017 (2019).
97. *Damiano Vesentini*: The Po Delta Biosphere Reserve: Management challenges and priorities deriving from anthropogenic pressure and sea level rise (2019).
98. *Emilie Arnesten*: Impacts of future sea level rise and high water on roads, railways and environmental objects: a GIS analysis of the potential effects of increasing sea levels and highest projected high water in Scania, Sweden (2019).
99. *Syed Muhammad Amir Raza*: Comparison of geospatial support in RDF stores: Evaluation for ICOS Carbon Portal metadata (2019).
100. *Hemin Tofiq*: Investigating the accuracy of Digital Elevation Models from UAV images in areas with low contrast: A sandy beach as a case study (2019).
101. *Evangelos Vafeiadis*: Exploring the distribution of accessibility by public transport using spatial analysis. A case study for retail concentrations and public hospitals in Athens (2019).
102. *Milan Sekulic*: Multi-Criteria GIS modelling for optimal alignment of roadway by-passes in the Tlokweng Planning Area, Botswana (2019).
103. *Ingrid Piirisaar*: A multi-criteria GIS analysis for siting of utility-scale photovoltaic solar plants in county Kilkenny, Ireland (2019).
104. *Nigel Fox*: Plant phenology and climate change: possible effect on the onset of various wild plant species' first flowering day in the UK (2019).
105. *Gunnar Hesch*: Linking conflict events and cropland development in Afghanistan, 2001 to 2011, using MODIS land cover data and Uppsala Conflict Data Programme (2019).

106. *Elijah Njoku*: Analysis of spatial-temporal pattern of Land Surface Temperature (LST) due to NDVI and elevation in Ilorin, Nigeria (2019).
107. *Katalin Bunyevácz*: Development of a GIS methodology to evaluate informal urban green areas for inclusion in a community governance program (2019).
108. *Paul dos Santos*: Automating synthetic trip data generation for an agent-based simulation of urban mobility (2019).
109. *Robert O' Dwyer*: Land cover changes in Southern Sweden from the mid-Holocene to present day: Insights for ecosystem service assessments (2019).
110. *Daniel Klingmyr*: Global scale patterns and trends in tropospheric NO<sub>2</sub> concentrations (2019).
111. *Marwa Farouk Elkabbany*: Sea Level Rise Vulnerability Assessment for Abu Dhabi, United Arab Emirates (2019).
112. *Jip Jan van Zoonen*: Aspects of Error Quantification and Evaluation in Digital Elevation Models for Glacier Surfaces (2020).
113. *Georgios Efthymiou*: The use of bicycles in a mid-sized city – benefits and obstacles identified using a questionnaire and GIS (2020).
114. *Haruna Olayiwola Jimoh*: Assessment of Urban Sprawl in MOWE/IBAFO Axis of Ogun State using GIS Capabilities (2020).
115. *Nikolaos Barmpas Zachariadis*: Development of an iOS, Augmented Reality for disaster management (2020).
116. *Ida Storm*: ICOS Atmospheric Stations: Spatial Characterization of CO<sub>2</sub> Footprint Areas and Evaluating the Uncertainties of Modelled CO<sub>2</sub> Concentrations (2020).
117. *Alon Zuta*: Evaluation of water stress mapping methods in vineyards using airborne thermal imaging (2020).
118. *Marcus Eriksson*: Evaluating structural landscape development in the municipality Upplands-Bro, using landscape metrics indices (2020).
119. *Ane Rahbek Vierø*: Connectivity for Cyclists? A Network Analysis of Copenhagen's Bike Lanes (2020).
120. *Cecilia Baggini*: Changes in habitat suitability for three declining Anatidae species in saltmarshes on the Mersey estuary, North-West England (2020).
121. *Bakrad Balabanian*: Transportation and Its Effect on Student Performance (2020).
122. *Ali Al Farid*: Knowledge and Data Driven Approaches for Hydrocarbon Microseepage Characterizations: An Application of Satellite Remote Sensing (2020).
123. *Bartłomiej Kolodziejczyk*: Distribution Modelling of Gene Drive-Modified Mosquitoes and Their Effects on Wild Populations (2020).
124. *Alexis Cazorla*: Decreasing organic nitrogen concentrations in European water bodies - links to organic carbon trends and land cover (2020).
125. *Kharid Mwakoba*: Remote sensing analysis of land cover/use conditions of community-based wildlife conservation areas in Tanzania (2021).
126. *Chinatsu Endo*: Remote Sensing Based Pre-Season Yellow Rust Early Warning in Oromia, Ethiopia (2021).
127. *Berit Mohr*: Using remote sensing and land abandonment as a proxy for long-term human out-migration. A Case Study: Al-Hassakeh Governorate, Syria (2021).

128. *Kanchana Nirmali Bandaranayake*: Considering future precipitation in delineation locations for water storage systems - Case study Sri Lanka (2021).
129. *Emma Bylund*: Dynamics of net primary production and food availability in the aftermath of the 2004 and 2007 desert locust outbreaks in Niger and Yemen (2021).
130. *Shawn Pace*: Urban infrastructure inundation risk from permanent sea-level rise scenarios in London (UK), Bangkok (Thailand) and Mumbai (India): A comparative analysis (2021).
131. *Oskar Evert Johansson*: The hydrodynamic impacts of Estuarine Oyster reefs, and the application of drone technology to this study (2021).
132. *Pritam Kumarsingh*: A Case Study to develop and test GIS/SDSS methods to assess the production capacity of a Cocoa Site in Trinidad and Tobago (2021).
133. *Muhammad Imran Khan*: Property Tax Mapping and Assessment using GIS (2021).
134. *Domna Kanari*: Mining geosocial data from Flickr to explore tourism patterns: The case study of Athens (2021).
135. *Mona Tykesson Klubien*: Livestock-MRSA in Danish pig farms (2021).
136. *Ove Njøten*: Comparing radar satellites. Use of Sentinel-1 leads to an increase in oil spill alerts in Norwegian waters (2021).
137. *Panagiotis Patrinos*: Change of heating fuel consumption patterns produced by the economic crisis in Greece (2021).
138. *Lukasz Langowski*: Assessing the suitability of using Sentinel-1A SAR multi-temporal imagery to detect fallow periods between rice crops (2021).
139. *Jonas Tillman*: Perception accuracy and user acceptance of legend designs for opacity data mapping in GIS (2022).
140. *Gabriela Olekszyk*: ALS (Airborne LIDAR) accuracy: Can potential low data quality of ground points be modelled/detected? Case study of 2016 LIDAR capture over Auckland, New Zealand (2022).